Supporting Information for

Ligand-Field-Dependent Behavior of meta-GGA Exchange in Transition-Metal Complex Spin-State Ordering

Efthymios I. Ioannidis[1] and Heather J. Kulik[1]

[1]Department of Chemical Engineering, Massachusetts Institute of Technology, Cambridge, MA 02139

Contents

Table S1. Ti(II) ion HS-LS total energies in Ha, spin-state splitting in kcal/mol with meta-GGA exchange percentage, slope (in kcal/mol/MGGAX), R^2 values for linear fits, NIST reference splitting in kcal/mol and error in kcal/mol.

	S1	S3	1-3	1-3 Error
0	-848.3482969422	-848.3680793715	-12.4	11.8
25	-848.4270005083	-848.4473135181	-12.7	11.5
50	-848.4985585314	-848.5193843543	-13.1	11.2
75	-848.5632254207	-848.5845506679	-13.4	10.8
100	-848.6211841303	-848.6430308387	-13.7	10.5
NIST			**-24.2**	
R^2	**1.00**	**1.00**	**1.00**	
Slope			**-1.29**	

Table S2. V(III) ion HS-LS total energies in Ha, spin-state splitting in kcal/mol with meta-GGA exchange percentage, slope (in kcal/mol/MGGAX), R^2 values for linear fits, NIST reference splitting in kcal/mol and error in kcal/mol.

	S1	S3	1-3	1-3 Error
0	-941.7468335080	-941.7707520652	-15.0	16.3
25	-941.8295782544	-941.8540855470	-15.4	16.0
50	-941.9048650915	-941.9299418946	-15.7	15.6
75	-941.9729593023	-941.9985928937	-16.1	15.2
100	-942.0340929472	-942.0602684827	-16.4	14.9
NIST			**-31.3**	
R^2	**1.00**	**1.00**	**1.00**	
Slope			**-1.42**	

Table S3. V(II) ion HS-LS total energies in Ha, spin-state splitting in kcal/mol with meta-GGA exchange percentage, slope (in kcal/mol/MGGAX), R^2 values for linear fits, NIST reference splitting in kcal/mol and error in kcal/mol.

	S2	S4	2-4	2-4 Error
0	-942.8347492916	-942.8718042289	-23.3	11.0
25	-942.9160114732	-942.9521208462	-22.7	11.6
50	-942.9907520760	-943.0250757879	-21.5	12.7
75	-943.0581305971	-943.0909395435	-20.6	13.6
100	-943.1190940378	-943.1499406512	-19.4	14.9
NIST			**-34.2**	
R^2	**1.00**	**1.00**	**0.99**	
Slope			**3.95**	

Table S4. Cr(III) ion HS-LS total energies in Ha, spin-state splitting in kcal/mol with meta-GGA exchange percentage, slope (in kcal/mol/MGGAX), R^2 values for linear fits, NIST reference splitting in kcal/mol and error in kcal/mol.

	S2	S4	2-4	2-4 Error
0	-1042.1157624089	-1042.1610601506	-28.4	14.6
25	-1042.2013635369	-1042.2447498716	-27.2	15.8
50	-1042.2797977568	-1042.3210689589	-25.9	17.1
75	-1042.3510650686	-1042.3900174127	-24.4	18.6
100	-1042.4151654727	-1042.4515952327	-22.9	20.2
NIST			-43.0	
R^2	**1.00**	**1.00**	**1.00**	
Slope			**5.56**	

Table S5. Cr(II) ion HS, IS, LS total energies in Ha, HS-LS/HS-IS spin-state splitting in kcal/mol with meta-GGA exchange percentage, slope (in kcal/mol/MGGAX), R^2 values for linear fits, NIST reference splitting in kcal/mol and error in kcal/mol.

	S1	Restricted S1	S3	S5	R1-5	3-5	R1-5 Error	3-5 Error
0	-1043.2584533327	-1043.1883569287	-1043.2724210532	-1043.3257985058	-86.2	-33.5	-14.4	14.5
25	-1043.3449336036	-1043.2740909614	-1043.3557470622	-1043.4061284926	-82.9	-31.6	-11.0	16.3
50	-1043.4237677674	-1043.3522531191	-1043.4316723959	-1043.4790972197	-79.6	-29.8	-7.7	18.2
75	-1043.4949558239	-1043.4228434019	-1043.5001970544	-1043.5447046871	-76.5	-27.9	-4.6	20.0
100	-1043.5584977734	-1043.4858618096	-1043.5613210376	-1043.6029508947	-73.5	-26.1	-1.6	21.8
NIST					-71.9	-48.0		
R^2	**1.00**	**1.00**	**1.00**	**1.00**	**1.00**	**1.00**		
Slope					**12.8**	**7.4**		

Table S6. Mn(III) ion HS, IS, LS (open shell and restricted) total energies in Ha, HS-IS spin-state splitting in kcal/mol with meta-GGA exchange percentage, slope (in kcal/mol/MGGAX), R^2 values for linear fits, NIST reference splitting in kcal/mol and error in kcal/mol. There is no experimentally characterized stable singlet so only HS-IS splitting error is calculated.

	S1	R-S1	S3	S5	R1-5	3-5	3-5 Error
0	-1148.5579839325	-1148.47213282076	-1148.5745468319	-1148.6363886569	-103.1	-38.8	20.2
25	-1148.6491105497	-1148.56230979237	-1148.6616461520	-1148.7211581756	-99.7	-37.3	21.7
50	-1148.7320769759	-1148.64468553297	-1148.7410061927	-1148.7978854654	-96.1	-35.7	23.4
75	-1148.7192010591	-1148.71926004256	-1148.8133351308	-1148.8665633155	-92.4	-33.4	25.7
100	-1148.7861023523	-1148.78603332116	-1148.8776971916	-1148.9271950869	-88.6	-31.1	28.0
NIST					-71.9	-59.1	
R^2	**0.89**	**1.00**	**1.00**	**1.00**	**1.00**	**0.99**	
Slope					**14.5**	**7.8**	

Table S7. Mn(II) ion HS, IS, LS total energies in Ha, HS-LS/HS-IS spin-state splitting in kcal/mol with meta-GGA exchange percentage, slope (in kcal/mol/MGGAX), R^2 values for linear fits, NIST reference splitting in kcal/mol and error in kcal/mol.

	S2	S4	S6	2-6	4-6	2-6 Error	4-6 Error
0	-1149.7014111123	-1149.8135435746	-1149.8951468660	-121.6	-51.2	26.4	25.5
25	-1149.7865673343	-1149.8973456422	-1149.9766041957	-119.2	-49.7	10.8	27.0
50	-1149.8642830858	-1149.9732699998	-1150.0502987216	-116.7	-48.3	1.3	28.4
75	-1149.9345598973	-1150.0416104013	-1150.1165290234	-114.2	-47.0	-2.2	29.7
100	-1149.9973923502	-1150.1026246908	-1150.1755492091	-111.8	-45.8	0.2	30.9
NIST				**-111.8**	**-76.7**		
R^2	**1.00**	**1.00**	**1.00**	**1.00**	**1.00**		
Slope				**9.8**	**5.4**		

Table S8. Fe(III) ion HS, IS, LS total energies in Ha, HS-LS/HS-IS spin-state splitting in kcal/mol with meta-GGA exchange percentage, slope (in kcal/mol/MGGAX), R^2 values for linear fits, NIST reference splitting in kcal/mol and error in kcal/mol.

	S2	S4	S6	2-6	4-6	2-6 Error	4-6 Error
0	-1261.1482260330	-1261.2354499877	-1261.3773852909	-143.8	-89.1	-9.2	3.1
25	-1261.2375979234	-1261.3215994213	-1261.4620247824	-140.8	-88.1	-6.2	4.1
50	-1261.3179698139	-1261.4001740129	-1261.5386408145	-138.5	-86.9	-3.9	5.3
75	-1261.3923417043	-1261.4711781566	-1261.6075426727	-135.0	-85.6	-0.4	6.6
100	-1261.4577135947	-1261.5346096616	-1261.6689935273	-132.6	-84.3	2.0	7.9
NIST				-134.6	-92.2		
R^2	**1.00**	**1.00**	**1.00**	**1.00**	**0.99**		
Slope				11.3	4.8		

Table S9. Fe(II) ion HS, IS, LS total energies in Ha, HS-LS/HS-IS spin-state splitting in kcal/mol with meta-GGA exchange percentage, slope (in kcal/mol/MGGAX), R^2 values for linear fits, NIST reference splitting in kcal/mol and error in kcal/mol.

	S1	R-S1	S3	S5	R1-5	3-5	R1-5 Error	3-5 Error
0	-1262.4664976745	-1262.3867769232	-1262.4798504763	-1262.5409234235	-96.7	-38.3	-9.9	17.2
25	-1262.5539152756	-1262.4736944057	-1262.5666769373	-1262.6247752686	-94.8	-36.5	-8.0	19.0
50	-1262.6332186048	-1262.5527214453	-1262.6456868399	-1262.7008848486	-93.0	-34.6	-6.2	20.8
75	-1262.7044076621	-1262.6238580421	-1262.7168801841	-1262.7692295456	-91.2	-32.8	-4.4	22.6
100	-1262.7674824475	-1262.6871041959	-1262.7802569698	-1262.8298090909	-89.5	-31.1	-2.8	24.4
NIST					**-86.8**	**-55.5**		
R^2	**1.00**	**1.00**	**1.00**	**1.00**	**1.00**	**1.00**		
Slope					**7.2**	**7.2**		

Table S10. Co(III) ion HS, IS, LS total energies in Ha, HS-LS/HS-IS spin-state splitting in kcal/mol with meta-GGA exchange percentage, slope (in kcal/mol/MGGAX), R^2 values for linear fits, NIST reference splitting in kcal/mol and error in kcal/mol.

	S1	R-S1	S3	S5	R1-5	3-5	R1-5 Error	3-5 Error
0	-1380.2181930897	-1380.12404406963	-1380.23346169937	-1380.3041049301	-113.0	-44.3	-10.2	21.1
25	-1380.3093713594	-1380.21441756368	-1380.32411546791	-1380.3915233049	-111.1	-42.3	-8.4	23.1
50	-1380.2967115861	-1380.29669203238	-1380.40661284346	-1380.4706044872	-109.1	-40.2	-6.4	25.3
75	-1380.3708040953	-1380.37086747578	-1380.48095382599	-1380.5416700118	-107.2	-38.1	-4.4	27.3
100	-1380.4370178070	-1380.43694389384	-1380.54713841551	-1380.6049939236	-105.5	-36.3	-2.7	29.1
NIST					**-102.8**	**-65.4**		
R^2	**0.92**	**1.00**	**1.00**	**1.00**	**1.00**	**1.00**		
Slope					**7.6**	**8.1**		

Table S11. Co(II) ion HS-LS total energies in Ha, spin-state splitting in kcal/mol with meta-GGA exchange percentage, slope (in kcal/mol/MGGAX), R^2 values for linear fits, NIST reference splitting in kcal/mol and error in kcal/mol.

	S2	S4	2-4	2-4 Error
0	-1381.5189421295	-1381.5563841589	-23.5	25.0
25	-1381.6055817535	-1381.6421460299	-22.9	25.6
50	-1381.6839028171	-1381.7195909223	-22.4	26.1
75	-1381.7542149245	-1381.7890397462	-21.9	26.7
100	-1381.8167822703	-1381.8507658069	-21.3	27.2
NIST			-48.5	
R^2	**1.00**	**1.00**	**1.00**	
Slope			**2.17**	

Table S12. Ni(III) ion HS-LS total energies in Ha, spin-state splitting in kcal/mol with meta-GGA exchange percentage, slope (in kcal/mol/MGGAX), R^2 values for linear fits, NIST reference splitting in kcal/mol and error in kcal/mol.

	S2	S4	2-4	2-4 Error
0	-1505.7011891020	-1505.7555880352	-34.1	22.6
25	-1505.7907279682	-1505.8463026569	-34.9	21.8
50	-1505.8720913765	-1505.9286607926	-35.5	21.2
75	-1505.9452793268	-1506.0026624419	-36.0	20.7
100	-1506.0102918191	-1506.0683076049	-36.4	20.3
NIST			**-56.7**	
R^2	**1.00**	**1.00**	**0.99**	
Slope			**-2.27**	

Table S13. Ni(II) ion HS-LS total energies in Ha, spin-state splitting in kcal/mol with meta-GGA exchange percentage, slope (in kcal/mol/MGGAX), R^2 values for linear fits, NIST reference splitting in kcal/mol and error in kcal/mol.

	S1	S3	1-3	1-3 Error
0	-1507.0513376679	-1507.0665689427	-9.6	30.6
25	-1507.1373004807	-1507.1531397904	-9.9	30.2
50	-1507.2147338563	-1507.2311616835	-10.3	29.8
75	-1507.2839730368	-1507.3009681867	-10.7	29.5
100	-1507.3453261239	-1507.3628439556	-11.0	29.1
NIST			**-40.1**	
R^2	**1.00**	**1.00**	**1.00**	
Slope			**-1.44**	

Table S14. Cu(III) ion HS-LS total energies in Ha, spin-state splitting in kcal/mol with meta-GGA exchange percentage, slope (in kcal/mol/MGGAX), R^2 values for linear fits, NIST reference splitting in kcal/mol and error in kcal/mol.

	S1	S3	1-3	1-3 Error
0	-1637.8008723988	-1637.8344249806	-21.1	25.4
25	-1637.8897984503	-1637.9244074292	-21.7	24.7
50	-1637.9699856948	-1638.0055898703	-22.3	24.1
75	-1638.0417454194	-1638.0783165262	-22.9	23.5
100	-1638.1053811827	-1638.1428809269	-23.5	22.9
NIST			**-46.5**	
R^2	**1.00**	**1.00**	**1.00**	
Slope			**-2.47**	

Table S15. SCAN splittings of transition metal ions and errors with respect to NIST references, all in kcal/mol. Calculations were carried out with Q-Chem 4.4 using the TZV basis set. Mean absolute error (MAE) and maximum error (MAX) presented for SCAN/TZV as assessed against NIST reference data and compared to TPSS errors reported in the text. The benchmark calculations using the SCAN[1] functional were performed in Q-Chem[2] using the same methodology as for the inorganic complexes with the default convergence thresholds.

	HS	LS	NIST	SCAN	Error	TPSS
Ti(II)	-848.6673235822	-848.6394836914	-24.2	-17.5	6.7	
V(III)	-942.0999137598	-942.0653090180	-31.4	-21.7	9.6	
V(II)	-943.1467253629	-943.1467253629	-34.1	-21.5	12.6	
Cr(III)	-1042.4838267192	-1042.4427841983	-43.1	-25.8	17.4	
Cr(II)	-1043.6534573567	-1043.5065756279	-71.9	-92.2	20.2	
Mn(II)	-1150.2355050898	-1150.1151906579	-111.8	-75.5	36.3	
Fe(III)	-1261.7365667439	-1261.4869250153	-134.4	-156.7	22.2	
Fe(II)	-1262.8738332533	-1262.7303641607	-86.7	-90.0	3.3	
Co(III)	-1380.6483782861	-1380.4856783028	-102.6	-102.1	0.5	
Co(II)	-1381.9061284742	-1381.8595776381	-48.4	-29.2	19.2	
Ni(III)	-1506.1094230850	-1506.0523457499	-56.7	-35.8	20.9	
Ni(II)	-1507.4275731036	-1507.3761553995	-39.9	-32.3	7.6	
Cu(III)	-1638.1484378417	-1638.1127410533	-46.4	-22.4	24.0	
H-L all (MAE)					15.4	12.9
H-L all (MAX)					36.3	29.1

Table S16. SCAN/TZV, M06-L/aug-cc-pVTZ, and TPSS/aug-cc-pVTZ splittings compared to literature CASPT2 results, all in kcal/mol.

$Fe(II)(L)_6$	TPSS	SCAN	M06-L	CASPT2
CO	71.5	68.3	47.6	47.7[3]
NH3	3.2	2.6	-8.5	-20.3[4]
H2O	-20.8	-26.4	-28.9	-46.6[4]

None	-89.5	-90.0	-87.6	-87.0[5]
MAE	18.9	16.7	7.6	--

Table S17. $[Ti(CO)_6]^{2+}$ HS-LS energies in Ha, spin-state splitting in kcal/mol with meta-GGA exchange, slope (in kcal/mol/MGGAX), and R^2 values for linear fits.

	HS	LS	ΔE (kcal/mol)
0	-1528.15110802231	-1528.14177869763	-5.85
10	-1528.28266358456	-1528.27325166025	-5.91
20	-1528.40887838918	-1528.39936268596	-5.97
30	-1528.52975243616	-1528.52011177477	-6.05
40	-1528.64528572548	-1528.63549892666	-6.14
50	-1528.75547825717	-1528.74552414163	-6.25
60	-1528.86033003121	-1528.85018741969	-6.36
70	-1528.95984104762	-1528.94948876085	-6.50
80	-1529.05401130637	-1529.04342816509	-6.64
90	-1529.14284080749	-1529.13200563242	-6.80
100	-1529.22632955095	-1529.21522116285	-6.97
R^2	**1.00**	**1.00**	**0.97**
Slope			**-1.1**

Table S18. $[V(CO)_6]^{3+}$ HS-LS energies in Ha, spin-state splitting in kcal/mol with meta-GGA exchange, slope (in kcal/mol/MGGAX), and R^2 values for linear fits.

	HS	LS	ΔE (kcal/mol)
0	-1622.01254224222	-1621.99674337355	-9.91
10	-1622.14482850632	-1622.12884469818	-10.03
20	-1622.27171210769	-1622.25556612287	-10.13

30	-1622.39319304633	-1622.37690764761	-10.22
40	-1622.50927132222	-1622.49286927241	-10.29
50	-1622.61994693536	-1622.60345099725	-10.35
60	-1622.72521988575	-1622.70865282216	-10.40
70	-1622.82509017340	-1622.80847474711	-10.43
80	-1622.91955779831	-1622.90291677211	-10.44
90	-1623.00862276049	-1622.99197889716	-10.44
100	-1623.09228505990	-1623.07566112227	-10.43
R^2	**1.00**	**1.00**	**0.87**
Slope			**-0.52**

Table S19. $[V(CO)_6]^{2+}$ HS-LS energies in Ha, spin-state splitting in kcal/mol with meta-GGA exchange, slope (in kcal/mol/MGGAX), and R^2 values for linear fits.

	HS	LS	ΔE (kcal/mol)
0	-1622.71256819846	-1622.69065186534	-13.75
10	-1622.84464100129	-1622.82269981079	-13.77
20	-1622.97135427553	-1622.94938005829	-13.79
30	-1623.09270802114	-1623.07069260785	-13.81
40	-1623.20870223815	-1623.18663745950	-13.85
50	-1623.31933692655	-1623.29721461322	-13.88
60	-1623.42461208634	-1623.40242406899	-13.92
70	-1623.52452771751	-1623.50226582684	-13.97
80	-1623.61908382009	-1623.59673988676	-14.02
90	-1623.70828039405	-1623.68584624874	-14.08
100	-1623.79211743940	-1623.76958491279	-14.14
R^2	**1.00**	**1.00**	**0.97**

Slope			**-0.39**

Table S20. $[Cr(CO)_6]^{3+}$ HS-LS energies in Ha, spin-state splitting in kcal/mol with meta-GGA exchange, slope (in kcal/mol/MGGAX), and R^2 values for linear fits.

	HS	LS	ΔE (kcal/mol)
0	-1722.49573489451	-1722.46176740469	-21.31
10	-1722.62829823019	-1722.59442029032	-21.26
20	-1722.75545839854	-1722.72167729835	-21.20
30	-1722.87721539950	-1722.84353842878	-21.13
40	-1722.99356923314	-1722.96000368159	-21.06
50	-1723.10451989940	-1723.07107305681	-20.99
60	-1723.21006739832	-1723.17674655442	-20.91
70	-1723.31021172988	-1723.27702417442	-20.83
80	-1723.40495289408	-1723.37190591682	-20.74
90	-1723.49429089092	-1723.46139178160	-20.64
100	-1723.57822572042	-1723.54548176878	-20.55
R^2	**1.00**	**1.00**	**0.99**
Slope			**0.77**

Table S21. $[Cr(CO)_6]^{2+}$ HS-LS energies in Ha, spin-state splitting in kcal/mol with meta-GGA exchange, slope (in kcal/mol/MGGAX), and R^2 values for linear fits.

	HS	LS	ΔE (kcal/mol)
0	-1723.12243845371	-1723.15406970649	19.85
10	-1723.25512442680	-1723.28635196999	19.60
20	-1723.38239820473	-1723.41328223691	19.38
30	-1723.50425978749	-1723.53486050726	19.20

40	-1723.62070917513	-1723.65108678104	19.06
50	-1723.73174636760	-1723.76196105826	18.96
60	-1723.83737136491	-1723.86748333890	18.90
70	-1723.93758416708	-1723.96765362297	18.87
80	-1724.03238477409	-1724.06247191047	18.88
90	-1724.12177318595	-1724.15193820140	18.93
100	-1724.20574940265	-1724.23605249576	19.02
R^2	**1.00**	**1.00**	**0.71**
Slope			**-0.83**

Table S22. $[Mn(CO)_6]^{3+}$ HS-LS energies in Ha, spin-state splitting in kcal/mol with meta-GGA exchange, slope (in kcal/mol/MGGAX), and R^2 values for linear fits.

	HS	LS	ΔE (kcal/mol)
0	-1828.96321983613	-1828.97363222444	6.53
10	-1829.09619680359	-1829.10635381942	6.37
20	-1829.22372095293	-1829.23369165759	6.26
30	-1829.34579228414	-1829.35564573897	6.18
40	-1829.46241079722	-1829.47221606353	6.15
50	-1829.57357649213	-1829.58340263130	6.17
60	-1829.67928936903	-1829.68920544227	6.22
70	-1829.77954942775	-1829.78962449641	6.32
80	-1829.87435666836	-1829.88465979377	6.47
90	-1829.96371109083	-1829.97431133431	6.65
100	-1830.04761269518	-1830.05857911805	6.88
R^2	**1.00**	**1.00**	**0.25**
Slope			**0.35**

Table S23. $[Mn(CO)_6]^{2+}$ HS-LS energies in Ha, spin-state splitting in kcal/mol with meta-GGA exchange, slope (in kcal/mol/MGGAX), and R^2 values for linear fits.

	HS	LS	ΔE (kcal/mol)
0	-1829.64592635745	-1829.70844027098	39.23
10	-1829.77944606467	-1829.84080454755	38.50
20	-1829.90749682337	-1829.96779996657	37.84
30	-1830.03007863356	-1830.08942652804	37.24
40	-1830.14719149524	-1830.20568423197	36.70
50	-1830.25883540839	-1830.31657307836	36.23
60	-1830.36501037304	-1830.42209306720	35.82
70	-1830.46571638917	-1830.52224419849	35.47
80	-1830.56095345679	-1830.61702647225	35.19
90	-1830.65072157589	-1830.70643988844	34.96
100	-1830.73502074648	-1830.79048444710	34.80
R^2	**1.00**	**1.00**	**0.96**
Slope			**-4.42**

Table S24. $[Fe(CO)_6]^{3+}$ HS-LS energies in Ha, spin-state splitting in kcal/mol with meta-GGA exchange, slope (in kcal/mol/MGGAX), and R^2 values for linear fits.

	HS	LS	ΔE (kcal/mol)
0	-1941.6417368874	-1941.7145163805	45.67
10	-1941.7754349858	-1941.8473087804	45.10
20	-1941.9036307388	-1941.9746826495	44.59
30	-1942.0263241466	-1942.0966379880	44.12

40	-1942.1435152091	-1942.2131747959	43.71
50	-1942.2552039263	-1942.3242930730	43.35
60	-1942.3613902983	-1942.4299928195	43.05
70	-1942.4620743248	-1942.5302740354	42.80
80	-1942.5572560061	-1942.6251367204	42.60
90	-1942.6469353421	-1942.7145808748	42.45
100	-1942.7311123328	-1942.7986064985	42.35
R^2	**1.00**	**1.00**	**0.95**
Slope			**-3.32**

Table S25. $[Fe(CO)_6]^{2+}$ HS-LS energies in Ha, spin-state splitting in kcal/mol with meta-GGA exchange, slope (in kcal/mol/MGGAX), and R^2 values for linear fits.

	HS	LS	ΔE (kcal/mol)
0	-1942.34203977686	-1942.46817786218	79.15
10	-1942.47604942104	-1942.60050158907	78.09
20	-1942.60456962437	-1942.72743923773	77.10
30	-1942.72760038688	-1942.84899080816	76.17
40	-1942.84514170850	-1942.96515630036	75.31
50	-1942.95719358930	-1943.07593571434	74.51
60	-1943.06375602925	-1943.18132905009	73.78
70	-1943.16482902836	-1943.28133630760	73.11
80	-1943.26041258663	-1943.37595748689	72.50
90	-1943.35050670405	-1943.46519258796	71.97
100	-1943.43511138062	-1943.54904161078	71.49
R^2	**1.00**	**1.00**	**0.99**
Slope			**-7.66**

Table S26. $[Co(CO)_6]^{3+}$ HS-LS energies in Ha, spin-state splitting in kcal/mol with meta-GGA exchange, slope (in kcal/mol/MGGAX), and R^2 values for linear fits.

	HS	LS	ΔE (kcal/mol)
0	-2060.66250285304	-2060.80184738770	87.44
10	-2060.79650095526	-2060.93450569725	86.60
20	-2060.92497513919	-2061.06172402104	85.81
30	-2061.04792540481	-2061.18350235906	85.07
40	-2061.16535175214	-2061.29984071129	84.39
50	-2061.27725418116	-2061.41073907776	83.76
60	-2061.38363269188	-2061.51619745845	83.18
70	-2061.48448728432	-2061.61621585337	82.66
80	-2061.57981795845	-2061.71079426252	82.19
90	-2061.66962471427	-2061.79993268590	81.77
100	-2061.75390755180	-2061.88363112351	81.40
R^2	**1.00**	**1.00**	**0.99**
Slope			**-6.04**

Table S27. $[Co(CO)_6]^{2+}$ HS-LS energies in Ha, spin-state splitting in kcal/mol with meta-GGA exchange, slope (in kcal/mol/MGGAX), and R^2 values for linear fits.

	HS	LS	ΔE (kcal/mol)
0	-2061.40374364365	-2061.46322347308	37.32
10	-2061.53829642179	-2061.59638748182	36.45
20	-2061.66734537464	-2061.72410176778	35.61
30	-2061.79089050220	-2061.84636633094	34.81

40	-2061.90893180448	-2061.96318117130	34.04
50	-2062.02146928144	-2062.07454628887	33.31
60	-2062.12850293312	-2062.18046168365	32.60
70	-2062.23003275951	-2062.28092735564	31.94
80	-2062.32605876061	-2062.37594330482	31.30
90	-2062.41658093641	-2062.46550953122	30.70
100	-2062.50159928692	-2062.54962603482	30.14
R^2	**1.00**	**1.00**	**1.00**
Slope			**-7.19**

Table S28. $[Ni(CO)_6]^{2+}$ HS-LS energies in Ha, spin-state splitting in kcal/mol with meta-GGA exchange, slope (in kcal/mol/MGGAX), and R^2 values for linear fits.

	HS	LS	DE(kcal/mol)
0	-2186.96688800699	-2186.95083188963	-10.08
10	-2187.10116402097	-2187.08476415775	-10.29
20	-2187.22992158741	-2187.21317956722	-10.51
30	-2187.35316070629	-2187.33607811807	-10.72
40	-2187.47088137763	-2187.45345981028	-10.93
50	-2187.58308360139	-2187.56532464386	-11.14
60	-2187.68976737762	-2187.67167261882	-11.35
70	-2187.79093270629	-2187.77250373512	-11.56
80	-2187.88657958741	-2187.86781799281	-11.77
90	-2187.97670802097	-2187.95761539186	-11.98
100	-2188.06131800699	-2188.04189593227	-12.19
R^2	**1.00**	**1.00**	**1.00**
Slope			**-2.11**

Table S29. $[Cu(CO)_6]^{3+}$ HS-LS energies in Ha, spin-state splitting in kcal/mol with meta-GGA exchange, slope (in kcal/mol/MGGAX), and R^2 values for linear fits.

	HS	LS	ΔE (kcal/mol)
0	-2318.36777420425	-2318.35890315158	-5.57
10	-2318.50158166210	-2318.49264693165	-5.61
20	-2318.62982205148	-2318.62080822411	-5.66
30	-2318.75249537237	-2318.74338702897	-5.72
40	-2318.86960162480	-2318.86038334622	-5.78
50	-2318.98114080875	-2318.97179717587	-5.86
60	-2319.08711292423	-2319.07762851789	-5.95
70	-2319.18751797124	-2319.17787737232	-6.05
80	-2319.28235594977	-2319.27254373914	-6.16
90	-2319.37162685984	-2319.36162761835	-6.27
100	-2319.45533070142	-2319.44512900996	-6.40
R^2	**0.99**	**0.99**	**0.97**
Slope			**-0.83**

Table S30. $[Ti(NH_3)_6]^{2+}$ HS-LS energies in Ha, spin-state splitting in kcal/mol with meta-GGA exchange, slope (in kcal/mol/MGGAX), and R^2 values for linear fits.

	HS	LS	ΔE (kcal/mol)
0	-1187.95682946153	-1187.93914289510	-11.10
10	-1188.04466474826	-1188.02779112167	-10.59
20	-1188.12906919347	-1188.11283745547	-10.19
30	-1188.21004279720	-1188.19428189650	-9.89
40	-1188.28758555944	-1188.27212444475	-9.70

50	-1188.36169748018	-1188.34636510023	-9.62
60	-1188.43237855944	-1188.41700386294	-9.65
70	-1188.49962879720	-1188.48404073286	-9.78
80	-1188.56344819347	-1188.54747571002	-10.02
90	-1188.62383674825	-1188.60730879440	-10.37
100	-1188.68079446153	-1188.66353998601	-10.83
R^2	**1.00**	**1.00**	**0.03**
Slope			**0.27**

Table S31. $[V(NH_3)_6]^{3+}$ HS-LS energies in Ha, spin-state splitting in kcal/mol with meta-GGA exchange, slope (in kcal/mol/MGGAX), and R^2 values for linear fits.

	HS	LS	ΔE (kcal/mol)
0	-1281.98575851235	-1281.96669571751	-11.96
10	-1282.07444494763	-1282.05520963831	-12.07
20	-1282.15967576135	-1282.14028243530	-12.17
30	-1282.24145095347	-1282.22191410849	-12.26
40	-1282.31977052403	-1282.30010465788	-12.34
50	-1282.39463447303	-1282.37485408349	-12.41
60	-1282.46604280045	-1282.44616238528	-12.48
70	-1282.53399550631	-1282.51402956326	-12.53
80	-1282.59849259059	-1282.57845561746	-12.57
90	-1282.65953405331	-1282.63944054785	-12.61
100	-1282.71711989445	-1282.69698435444	-12.64
R^2	**1.00**	**1.00**	**0.97**
Slope			**-0.67**

Table S32. $[V(NH_3)_6]^{2+}$ HS-LS energies in Ha, spin-state splitting in kcal/mol with meta-GGA exchange, slope (in kcal/mol/MGGAX), and R^2 values for linear fits.

	HS	LS	ΔE (kcal/mol)
0	-1282.50932680436	-1282.47736253231	-20.06
10	-1282.59792316601	-1282.56610866300	-19.96
20	-1282.68305910166	-1282.65137545505	-19.88
30	-1282.76473461131	-1282.73316290847	-19.81
40	-1282.84294969495	-1282.81147102325	-19.75
50	-1282.91770435261	-1282.88629979940	-19.71
60	-1282.98899858425	-1282.95764923691	-19.67
70	-1283.05683238990	-1283.02551933579	-19.65
80	-1283.12120576955	-1283.08991009601	-19.64
90	-1283.18211872320	-1283.15082151760	-19.64
100	-1283.23957125085	-1283.20825360056	-19.65
R^2	**1.00**	**1.00**	**0.86**
Slope			**0.41**

Table S33. $[Cr(NH_3)_6]^{3+}$ HS-LS energies in Ha, spin-state splitting in kcal/mol with meta-GGA exchange, slope (in kcal/mol/MGGAX), and R^2 values for linear fits.

	HS	LS	ΔE (kcal/mol)
0	-1382.46385703741	-1382.42471677624	-24.56
10	-1382.55309277416	-1382.51436158682	-24.30
20	-1382.63884135008	-1382.60047517460	-24.07
30	-1382.72110276518	-1382.68305753960	-23.87
40	-1382.79987701943	-1382.76210868180	-23.70

50	-1382.87516411286	-1382.83762860121	-23.55
60	-1382.94696404545	-1382.90961729783	-23.44
70	-1383.01527681722	-1382.97807477167	-23.34
80	-1383.08010242816	-1383.04300102270	-23.28
90	-1383.14144087827	-1383.10439605095	-23.25
100	-1383.19929216754	-1383.16225985641	-23.24
R^2	**1.00**	**1.00**	**0.92**
Slope			**1.32**

Table S34. $[Cr(NH_3)_6]^{2+}$ HS-LS energies in Ha, spin-state splitting in kcal/mol with meta-GGA exchange, slope (in kcal/mol/MGGAX), and R^2 values for linear fits.

	HS	LS	ΔE (kcal/mol)
0	-1382.95024958301	-1382.90781727278	-26.63
10	-1383.03902541675	-1382.99918271652	-25.00
20	-1383.12430835410	-1383.08683459796	-23.51
30	-1383.20609839507	-1383.17077291708	-22.17
40	-1383.28439553966	-1383.25099767390	-20.96
50	-1383.35919978786	-1383.32750886841	-19.89
60	-1383.43051113968	-1383.40030650061	-18.95
70	-1383.49832959511	-1383.46939057049	-18.16
80	-1383.56265515416	-1383.53476107807	-17.50
90	-1383.62348781683	-1383.59641802334	-16.99
100	-1383.68082758312	-1383.65436140630	-16.61
R^2	**1.00**	**1.00**	**0.96**
Slope			**10.02**

Table S35. $[Mn(NH_3)_6]^{2+}$ HS-LS energies in Ha, spin-state splitting in kcal/mol with meta-GGA exchange, slope (in kcal/mol/MGGAX), and R^2 values for linear fits.

	HS	LS	DE(kcal/mol)
0	-1489.48655922290	-1489.43788553922	-30.54
10	-1489.57584002364	-1489.52845786717	-29.73
20	-1489.66158701275	-1489.61550592410	-28.92
30	-1489.74380019022	-1489.69902971001	-28.09
40	-1489.82247955603	-1489.77902922490	-27.27
50	-1489.89762511021	-1489.85550446876	-26.43
60	-1489.96923685274	-1489.92845544160	-25.59
70	-1490.03731478363	-1489.99788214342	-24.74
80	-1490.10185890288	-1490.06378457423	-23.89
90	-1490.16286921049	-1490.12616273399	-23.03
100	-1490.22034570645	-1490.18501662274	-22.17
R^2	**1.00**	**1.00**	**1.00**
Slope			**8.37**

Table S36. $[Fe(NH_3)_6]^{3+}$ HS-LS energies in Ha, spin-state splitting in kcal/mol with meta-GGA exchange, slope (in kcal/mol/MGGAX), and R^2 values for linear fits.

	HS	LS	DE(kcal/mol)
0	-1601.62372318711	-1601.64348549088	12.40
10	-1601.71366410704	-1601.73417541217	12.87
20	-1601.80003845080	-1601.82132165708	13.36
30	-1601.88284621839	-1601.90492422560	13.85
40	-1601.96208740981	-1601.98498311775	14.37
50	-1602.03776202505	-1602.06149833351	14.89
60	-1602.10987006412	-1602.13446987288	15.44

70	-1602.17841152702	-1602.20389773587	15.99
80	-1602.24338641375	-1602.26978192248	16.56
90	-1602.30479472430	-1602.33212243270	17.15
100	-1602.36263645869	-1602.39091926654	17.75
	1.00	**1.00**	**1.00**
			5.35

Table S37. $[Fe(NH_3)_6]^{2+}$ HS-LS energies in Ha, spin-state splitting in kcal/mol with meta-GGA exchange, slope (in kcal/mol/MGGAX), and R^2 values for linear fits.

	HS	LS	ΔE (kcal/mol)
0	-1602.17409351418	-1602.17136701502	-1.71
10	-1602.26418276714	-1602.26214717545	-1.28
20	-1602.35069995150	-1602.34937649864	-0.83
30	-1602.43364506727	-1602.43305498461	-0.37
40	-1602.51301811442	-1602.51318263335	0.10
50	-1602.58881909297	-1602.58975944487	0.59
60	-1602.66104800291	-1602.66278541915	1.09
70	-1602.72970484426	-1602.73226055621	1.60
80	-1602.79478961700	-1602.79818485603	2.13
90	-1602.85630232114	-1602.86055831862	2.67
100	-1602.91424295667	-1602.91938094399	3.22
R^2	**1.00**	**1.00**	**1.00**
Slope			**4.93**

Table S38. $[Co(NH_3)_6]^{3+}$ HS-LS energies in Ha, spin-state splitting in kcal/mol with meta-GGA exchange, slope (in kcal/mol/MGGAX), and R^2 values for linear fits.

	HS	LS	ΔE (kcal/mol)
0	-1720.64420389193	-1720.71563323221	44.82
10	-1720.73466167873	-1720.80637692787	45.00
20	-1720.82146754585	-1720.89354961159	45.23
30	-1720.90462149330	-1720.97715128338	45.51
40	-1720.98412352109	-1721.05718194322	45.84
50	-1721.05997362918	-1721.13364159112	46.23
60	-1721.13217181761	-1721.20653022708	46.66
70	-1721.20071808635	-1721.27584785112	47.14
80	-1721.26561243543	-1721.34159446319	47.68
90	-1721.32685486483	-1721.40377006333	48.26
100	-1721.38444537455	-1721.46237465154	48.90
R^2	**1.00**	**1.00**	**0.97**
Slope			**4.08**

Table S39. $[Co(NH_3)_6]^{2+}$ HS-LS energies in Ha, spin-state splitting in kcal/mol with meta-GGA exchange, slope (in kcal/mol/MGGAX), and R^2 values for linear fits.

	HS	LS	ΔE (kcal/mol)
0	-1721.23036071826	-1721.22960733192	-0.47
10	-1721.32135214336	-1721.32024772241	-0.69
20	-1721.40873895717	-1721.40730119809	-0.90
30	-1721.49252115964	-1721.49076775896	-1.10
40	-1721.57269875083	-1721.57064740503	-1.29
50	-1721.64927173070	-1721.64694013626	-1.46

60	-1721.72224009928	-1721.71964595269	-1.63
70	-1721.79160385654	-1721.78876485430	-1.78
80	-1721.85736300250	-1721.85429684111	-1.92
90	-1721.91951753716	-1721.91624191310	-2.06
100	-1721.97806746051	-1721.97460007028	-2.18
R^2	**1.00**	**1.00**	**0.99**
Slope			**-1.70**

Table S40. $[Ni(NH_3)_6]^{2+}$ HS-LS energies in Ha, spin-state splitting in kcal/mol with meta-GGA exchange, slope (in kcal/mol/MGGAX), and R^2 values for linear fits.

	HS	LS	ΔE (kcal/mol)
0	-1846.78517339860	-1846.76567352447	-12.24
10	-1846.87607488671	-1846.85622728251	-12.45
20	-1846.96334871283	-1846.94315547412	-12.67
30	-1847.04699487692	-1847.02645809930	-12.89
40	-1847.12701337902	-1847.10613515804	-13.10
50	-1847.20340421911	-1847.18218665034	-13.31
60	-1847.27616739720	-1847.25461257623	-13.53
70	-1847.34530291328	-1847.32341293566	-13.74
80	-1847.41081076736	-1847.38858772867	-13.95
90	-1847.47269095944	-1847.45013695524	-14.15
100	-1847.53094348951	-1847.50806061538	-14.36
R^2	**1.00**	**1.00**	**1.00**
Slope			**-2.12**

Table S41. $[Cu(NH_3)_6]^{3+}$ HS-LS energies in Ha, spin-state splitting in kcal/mol with meta-GGA exchange, slope (in kcal/mol/MGGAX), and R^2 values for linear fits.

	HS	LS	ΔE (kcal/mol)
0	-1978.34330424894	-1978.33388236746	-5.91
10	-1978.43390528046	-1978.42429457684	-6.03
20	-1978.52085395105	-1978.51105421937	-6.15
30	-1978.60415026072	-1978.59416129507	-6.27
40	-1978.68379420944	-1978.67361580393	-6.39
50	-1978.75978579725	-1978.74941774594	-6.51
60	-1978.83212502413	-1978.82156712113	-6.63
70	-1978.90081189008	-1978.89006392945	-6.74
80	-1978.96584639511	-1978.95490817095	-6.86
90	-1979.02722853920	-1979.01609984560	-6.98
100	-1979.08495832237	-1979.07363895341	-7.10
R^2	**1.00**	**1.00**	**1.00**
Slope			**-1.19**

Table S42. $[Ti(H_2O)_6]^{2+}$ HS-LS energies in Ha, spin-state splitting in kcal/mol with meta-GGA exchange, slope (in kcal/mol/MGGAX), and R^2 values for linear fits.

	HS	LS	ΔE (kcal/mol)
0	-1307.12494641769	-1307.10778718584	-10.77
10	-1307.21843927367	-1307.20093414462	-10.98
20	-1307.30831825038	-1307.29051412263	-11.17
30	-1307.39458334783	-1307.37652711985	-11.33
40	-1307.47723456599	-1307.45897313630	-11.46
50	-1307.55627190489	-1307.53785217199	-11.56

60	-1307.63169536451	-1307.61316422688	-11.63
70	-1307.70350494486	-1307.68490930100	-11.67
80	-1307.77170064593	-1307.75308739434	-11.68
90	-1307.83628246774	-1307.81769850691	-11.66
100	-1307.89725041027	-1307.87874263870	-11.61
R^2	**1.00**	**1.00**	**0.81**
Slope			**-0.85**

Table S43. $[V(H_2O)_6]^{3+}$ HS-LS energies in Ha, spin-state splitting in kcal/mol with meta-GGA exchange, slope (in kcal/mol/MGGAX), and R^2 values for linear fits.

	HS	LS	ΔE (kcal/mol)
0	-1401.1044699820	-1401.0860797640	-11.54
10	-1401.1992492524	-1401.1808072001	-11.57
20	-1401.2901819555	-1401.2717092832	-11.59
30	-1401.3773276697	-1401.3588220075	-11.61
40	-1401.4607609815	-1401.4422137267	-11.64
50	-1401.5405087329	-1401.5219003147	-11.68
60	-1401.6166183736	-1401.5979450704	-11.72
70	-1401.6891297562	-1401.6704046556	-11.75
80	-1401.7580693432	-1401.7392518793	-11.81
90	-1401.8234860864	-1401.8046092440	-11.85
100	-1401.8853981750	-1401.8664372089	-11.90
R^2	**1.00**	**1.00**	**0.98**
Slope			**-0.35**

Table S44. $[V(H_2O)_6]^{2+}$ HS-LS energies in Ha, spin-state splitting in kcal/mol with meta-GGA exchange, slope (in kcal/mol/MGGAX), and R^2 values for linear fits.

	HS	LS	ΔE (kcal/mol)
0	-1401.66228156720	-1401.62889086537	-20.95
10	-1401.75659492194	-1401.72267211261	-21.29
20	-1401.84723913701	-1401.81294583999	-21.52
30	-1401.93421421241	-1401.89971204753	-21.65
40	-1402.01752014815	-1401.98297073522	-21.68
50	-1402.09715694420	-1402.06272190305	-21.61
60	-1402.17312460060	-1402.13896555104	-21.43
70	-1402.24542311732	-1402.21170167919	-21.16
80	-1402.31405249438	-1402.28093028746	-20.78
90	-1402.37901273176	-1402.34665137590	-20.31
100	-1402.44030382948	-1402.40886494449	-19.73
R^2	**1.00**	**1.00**	**0.43**
Slope			**1.22**

Table S45. $[Cr(H_2O)_6]^{3+}$ HS-LS energies in Ha, spin-state splitting in kcal/mol with meta-GGA exchange, slope (in kcal/mol/MGGAX), and R^2 values for linear fits.

	HS	LS	ΔE (kcal/mol)
0	-1501.55440267872	-1501.51793109285	-22.89
10	-1501.64946825516	-1501.61343258400	-22.61
20	-1501.74085573980	-1501.70523048118	-22.35
30	-1501.82856513268	-1501.79332478437	-22.11

40	-1501.91259643379	-1501.87771549358	-21.89
50	-1501.99294964312	-1501.95840260881	-21.68
60	-1502.06962476067	-1502.03538613005	-21.48
70	-1502.14262178645	-1502.10866605732	-21.31
80	-1502.21194072045	-1502.17824239059	-21.15
90	-1502.27758156268	-1502.24411512989	-21.00
100	-1502.33954431313	-1502.30628427520	-20.87
R^2	**1.00**	**1.00**	**0.99**
Slope			**2.02**

Table S46. $[Cr(H_2O)_6]^{2+}$ HS-LS energies in Ha, spin-state splitting in kcal/mol with meta-GGA exchange, slope (in kcal/mol/MGGAX), and R^2 values for linear fits.

	HS	LS	ΔE (kcal/mol)
0	-1502.10298872984	-1502.05467958285	-30.31
10	-1502.19741154194	-1502.15132778531	-28.92
20	-1502.28814262583	-1502.24410375192	-27.63
30	-1502.37518198151	-1502.33300748269	-26.46
40	-1502.45852960896	-1502.41803897761	-25.41
50	-1502.53818550821	-1502.49919823669	-24.46
60	-1502.61414967925	-1502.57648525995	-23.63
70	-1502.68642212207	-1502.64990004733	-22.92
80	-1502.75500283668	-1502.71944259889	-22.31
90	-1502.81989182308	-1502.78511291460	-21.82
100	-1502.88108908127	-1502.84691099447	-21.45
R^2	**1.00**	**1.00**	**0.97**
Slope			**8.87**

Table S47. $[Mn(H_2O)_6]^{3+}$ HS-LS energies in Ha, spin-state splitting in kcal/mol with meta-GGA exchange, slope (in kcal/mol/MGGAX), and R^2 values for linear fits.

	HS	LS	ΔE (kcal/mol)
0	-1608.03276209999	-1607.99467638389	-23.90
10	-1608.12786135195	-1608.09158868047	-22.76
20	-1608.21925006707	-1608.18472320159	-21.67
30	-1608.30692824534	-1608.27407994723	-20.61
40	-1608.39089588675	-1608.35965891740	-19.60
50	-1608.47115299131	-1608.44146011210	-18.63
60	-1608.54769955903	-1608.51948353134	-17.71
70	-1608.62053558990	-1608.59372917508	-16.82
80	-1608.68966108392	-1608.66419704336	-15.98
90	-1608.75507604109	-1608.73088713618	-15.18
100	-1608.81678046141	-1608.79379945351	-14.42
R^2	**1.00**	**1.00**	**1.00**
Slope			**9.48**

Table S48. $[Mn(H_2O)_6]^{2+}$ HS-LS energies in Ha, spin-state splitting in kcal/mol with meta-GGA exchange, slope (in kcal/mol/MGGAX), and R^2 values for linear fits.

	HS	LS	ΔE (kcal/mol)
0	-1608.65167490726	-1608.56714061296	-53.05
10	-1608.74649745219	-1608.66367304071	-51.97
20	-1608.83759041929	-1608.75643282680	-50.93
30	-1608.92495380854	-1608.84541997122	-49.91
40	-1609.00858761993	-1608.93063447399	-48.92
50	-1609.08849185348	-1609.01207633509	-47.95
60	-1609.16466650919	-1609.08974555453	-47.01

70	-1609.23711158705	-1609.16364213230	-46.10
80	-1609.30582708706	-1609.23376606843	-45.22
90	-1609.37081300923	-1609.30011736287	-44.36
100	-1609.43206935355	-1609.36269601567	-43.53
R^2	**1.00**	**1.00**	**1.00**
Slope			**9.51**

Table S49. $[Fe(H_2O)_6]^{3+}$ HS-LS energies in Ha, spin-state splitting in kcal/mol with meta-GGA exchange, slope (in kcal/mol/MGGAX), and R^2 values for linear fits.

	HS	LS	ΔE (kcal/mol)
0	-1720.73879954386	-1720.69711280931	-26.16
10	-1720.83413792719	-1720.79389127333	-25.25
20	-1720.92572800336	-1720.88692915381	-24.35
30	-1721.01356977239	-1720.97622645075	-23.43
40	-1721.09766323424	-1721.06178316415	-22.51
50	-1721.17800838895	-1721.14359929402	-21.59
60	-1721.25460523650	-1721.22167484033	-20.66
70	-1721.32745377690	-1721.29600980311	-19.73
80	-1721.39655401014	-1721.36660418236	-18.79
90	-1721.46190593623	-1721.43345797806	-17.85
100	-1721.52350955516	-1721.49657119023	-16.90
R^2	**1.00**	**1.00**	**1.00**
Slope			**9.25**

Table S50. $[Fe(H_2O)_6]^{2+}$ HS-LS energies in Ha, spin-state splitting in kcal/mol with meta-GGA exchange, slope (in kcal/mol/MGGAX), and R^2 values for linear fits.

	HS	LS	ΔE (kcal/mol)
0	-1721.32869582112	-1721.28574512712	-26.95
10	-1721.42443860176	-1721.38239206584	-26.38
20	-1721.51641094403	-1721.47528662013	-25.81
30	-1721.60461284793	-1721.56442878999	-25.22
40	-1721.68904431347	-1721.64981857541	-24.61
50	-1721.76970534062	-1721.73145597640	-24.00
60	-1721.84659592942	-1721.80934099297	-23.38
70	-1721.91971607984	-1721.88347362509	-22.74
80	-1721.98906579189	-1721.95385387278	-22.10
90	-1722.05464506558	-1722.02048173604	-21.44
100	-1722.11645390089	-1722.08335721487	-20.77
R^2	**1.00**	**1.00**	**1.00**
Slope			**6.18**

Table S51. $[Co(H_2O)_6]^{3+}$ HS-LS energies in Ha, spin-state splitting in kcal/mol with meta-GGA exchange, slope (in kcal/mol/MGGAX), and R^2 values for linear fits.

	HS	LS	ΔE (kcal/mol)
0	-1839.74648933767	-1839.74601582080	-0.30
10	-1839.84248478037	-1839.84275956362	0.17
20	-1839.93469730502	-1839.93573504388	0.65
30	-1840.02312691161	-1840.02494226159	1.14
40	-1840.10777360014	-1840.11038121674	1.64

50	-1840.18863737060	-1840.19205190933	2.14
60	-1840.26571822302	-1840.26995433936	2.66
70	-1840.33901615736	-1840.34408850684	3.18
80	-1840.40853117365	-1840.41445441175	3.72
90	-1840.47426327187	-1840.48105205412	4.26
100	-1840.53621245204	-1840.54388143392	4.81
R^2	**1.00**	**1.00**	**1.00**
Slope			**5.11**

Table S52. $[Co(H_2O)_6]^{2+}$ HS-LS energies in Ha, spin-state splitting in kcal/mol with meta-GGA exchange, slope (in kcal/mol/MGGAX), and R^2 values for linear fits.

	HS	LS	ΔE (kcal/mol)
0	-1840.38076857131	-1840.34931084008	-19.74
10	-1840.47742139531	-1840.44578384210	-19.85
20	-1840.57027067979	-1840.53846675571	-19.96
30	-1840.65931642474	-1840.62735958092	-20.05
40	-1840.74455863015	-1840.71246231772	-20.14
50	-1840.82599729603	-1840.79377496613	-20.22
60	-1840.90363242239	-1840.87129752613	-20.29
70	-1840.97746400922	-1840.94502999771	-20.35
80	-1841.04749205651	-1841.01497238090	-20.41
90	-1841.11371656428	-1841.08112467568	-20.45
100	-1841.17613753252	-1841.14348688206	-20.49
R^2	**1.00**	**1.00**	**0.98**
Slope			**-0.75**

Table S53. $[Ni(H_2O)_6]^{3+}$ HS-LS energies in Ha, spin-state splitting in kcal/mol with meta-GGA exchange, slope (in kcal/mol/MGGAX), and R^2 values for linear fits.

	HS	LS	ΔE (kcal/mol)
0	-1965.25736575469	-1965.25745312653	0.05
10	-1965.35375185385	-1965.35386151671	0.07
20	-1965.44632442759	-1965.44646451618	0.09
30	-1965.53508347590	-1965.53526212495	0.11
40	-1965.62002899881	-1965.62025434302	0.14
50	-1965.70116099627	-1965.70144117038	0.18
60	-1965.77847946833	-1965.77882260705	0.22
70	-1965.85198441496	-1965.85239865300	0.26
80	-1965.92167583617	-1965.92216930826	0.31
90	-1965.98755373196	-1965.98813457281	0.36
100	-1966.04961810232	-1966.05029444666	0.42
R^2	**1.00**	**1.00**	**0.96**
Slope			**0.37**

Table S54. $[Ni(H_2O)_6]^{2+}$ HS-LS energies in Ha, spin-state splitting in kcal/mol with meta-GGA exchange, slope (in kcal/mol/MGGAX), and R^2 values for linear fits.

	HS	LS	ΔE (kcal/mol)
0	-1965.92028909126	-1965.89764938661	-14.21
10	-1966.01696465886	-1965.99392479038	-14.46
20	-1966.10981206406	-1966.08637838152	-14.70
30	-1966.19883130681	-1966.17501016005	-14.95
40	-1966.28402238716	-1966.25982012595	-15.19

50	-1966.36538530510	-1966.34080827924	-15.42
60	-1966.44292006062	-1966.41797461990	-15.65
70	-1966.51662665373	-1966.49131914795	-15.88
80	-1966.58650508442	-1966.56084186336	-16.10
90	-1966.65255535269	-1966.62654276616	-16.32
100	-1966.71477745855	-1966.68842185634	-16.54
R^2	**1.00**	**1.00**	**1.00**
Slope			**-2.33**

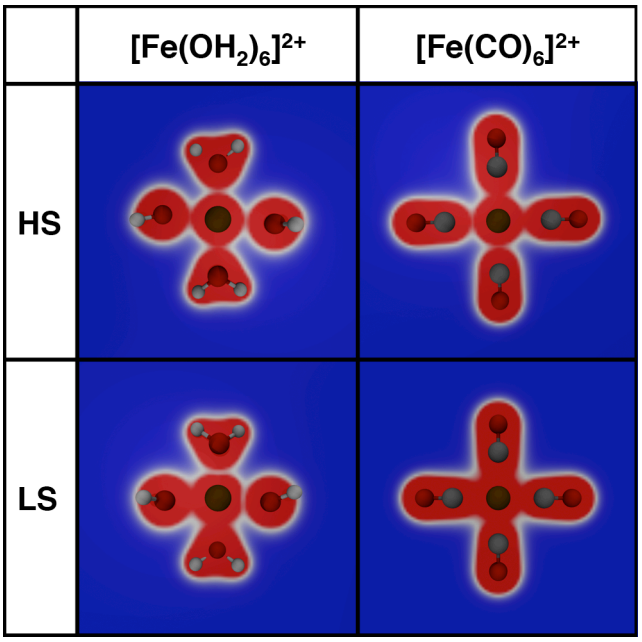

Figure S1. Cuts of the total electron density in the equatorial plane of $[Fe(OH_2)_6]^{2+}$ (left) and $[Fe(CO)_6]^{2+}$ right in high-spin (top) and low-spin (bottom) configurations. The white border indicates an isosurface of 0.06 e, red shading indicates density values higher than that isosurface value, and blue density values below that isosurface value. Iron atoms (brown), carbon atoms (gray), oxygen atoms (red), and hydrogen atoms (white) in the equatorial plane are shown as balls and sticks.

Table S55. S^2 values of open-shell singlet complexes.

M^{q+}	CO	NH_3	H_2O
Ti^{2+}	1.0	1.0	1.0
V^{3+}	1.0	1.0	--

Cr^{2+}	1.0	1.0-1.4	1.0
Mn^{3+}	1.0	1.2	1.0
Fe^{2+}	0.0	0.0	0.0
Co^{3+}	0.0	0.0	0.0
Ni^{2+}	0.0	1.0	1.0
Cu^{3+}	1.0	1.2	--

Table S56. $[Fe(PH_3)_6]^{2+}$ HS-LS energies in Ha, spin-state splitting in kcal/mol with meta-GGA exchange, slope (in kcal/mol/MGGAX), and R^2 values for linear fits.

	HS	LS	ΔE (kcal/mol)
0	-3320.5459003102	-3320.6060310216	37.71
10	-3320.7188031022	-3320.7779031022	37.07
20	-3320.8855062043	-3320.9436062043	36.47
30	-3321.0460093065	-3321.1032093065	35.91
40	-3321.2003124086	-3321.2566124086	35.38
50	-3321.3484155108	-3321.4040155108	34.89
60	-3321.4903186130	-3321.5451186130	34.44
70	-3321.6260217151	-3321.6802217151	34.03
80	-3321.7555248173	-3321.8091248173	33.65
90	-3321.8788279194	-3321.9319279194	33.31
100	-3321.9959300910	-3322.0485310216	33.01
R^2	**1.00**	**1.00**	**0.99**
Slope			**-4.70**

Table S57. $[Fe(PH_3)_6]^{3+}$ HS-LS energies in Ha, spin-state splitting in kcal/mol with meta-GGA exchange, slope (in kcal/mol/MGGAX), and R^2 values for linear fits.

	HS	LS	ΔE (kcal/mol)
0	-3320.01240678200	-3320.05267192800	25.27
10	-3320.18504591384	-3320.22493787225	25.03

20	-3320.35144547033	-3320.39101365114	24.83
30	-3320.51160545145	-3320.55089926468	24.66
40	-3320.66552585720	-3320.70459471287	24.52
50	-3320.81320668760	-3320.85209999569	24.41
60	-3320.95464794262	-3320.99341511317	24.33
70	-3321.08984962229	-3321.12854006528	24.28
80	-3321.21881172659	-3321.25747485204	24.26
90	-3321.34153425552	-3321.38021947345	24.28
100	-3321.45801720910	-3321.49677392950	24.32
R^2	**1.00**	**1.00**	**0.83**
Slope			**-0.95**

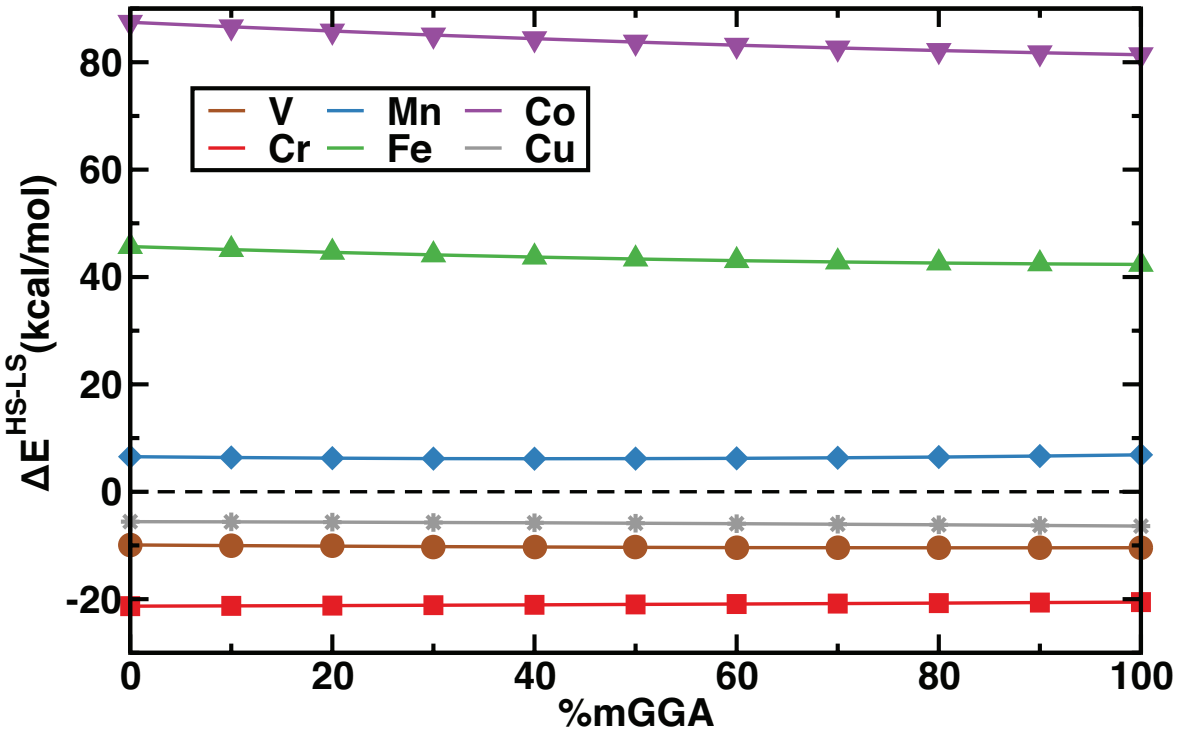

Figure S2. $[M(CO)_6]^{3+}$ splittings with percentage of meta-GGA exchange.

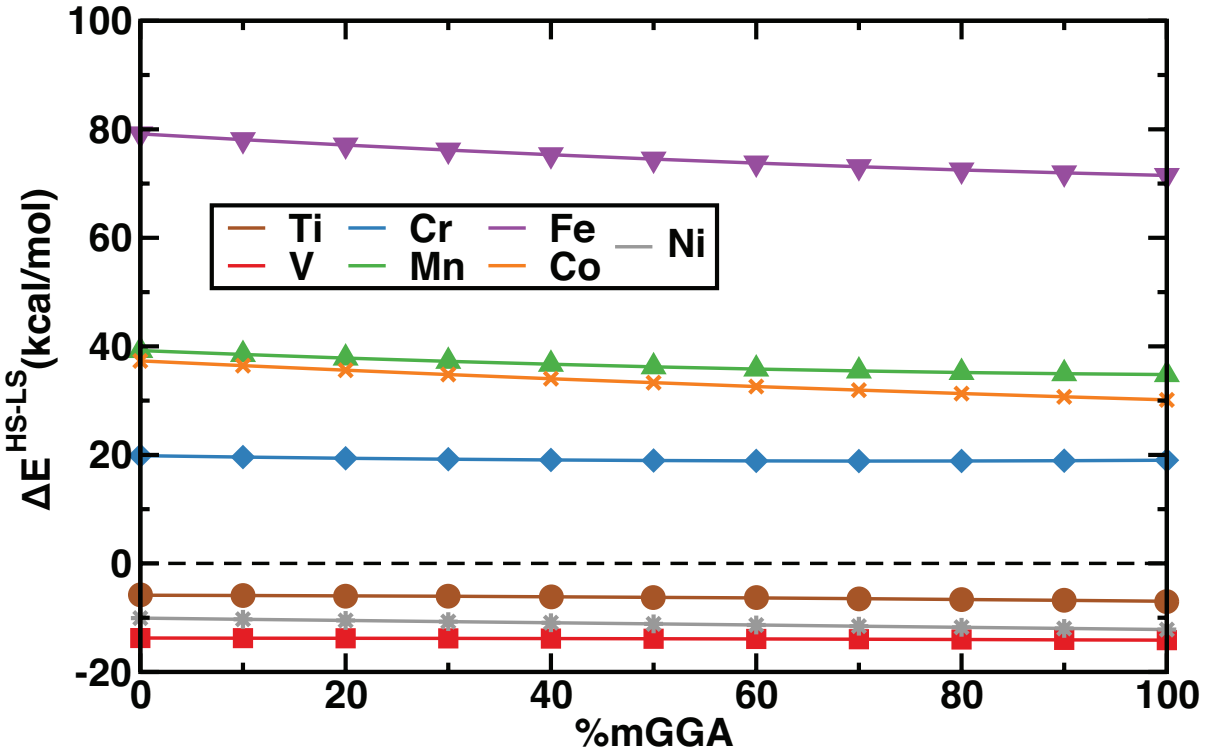

Figure S3. $[M(CO)_6]^{2+}$ splittings with percentage of meta-GGA exchange.

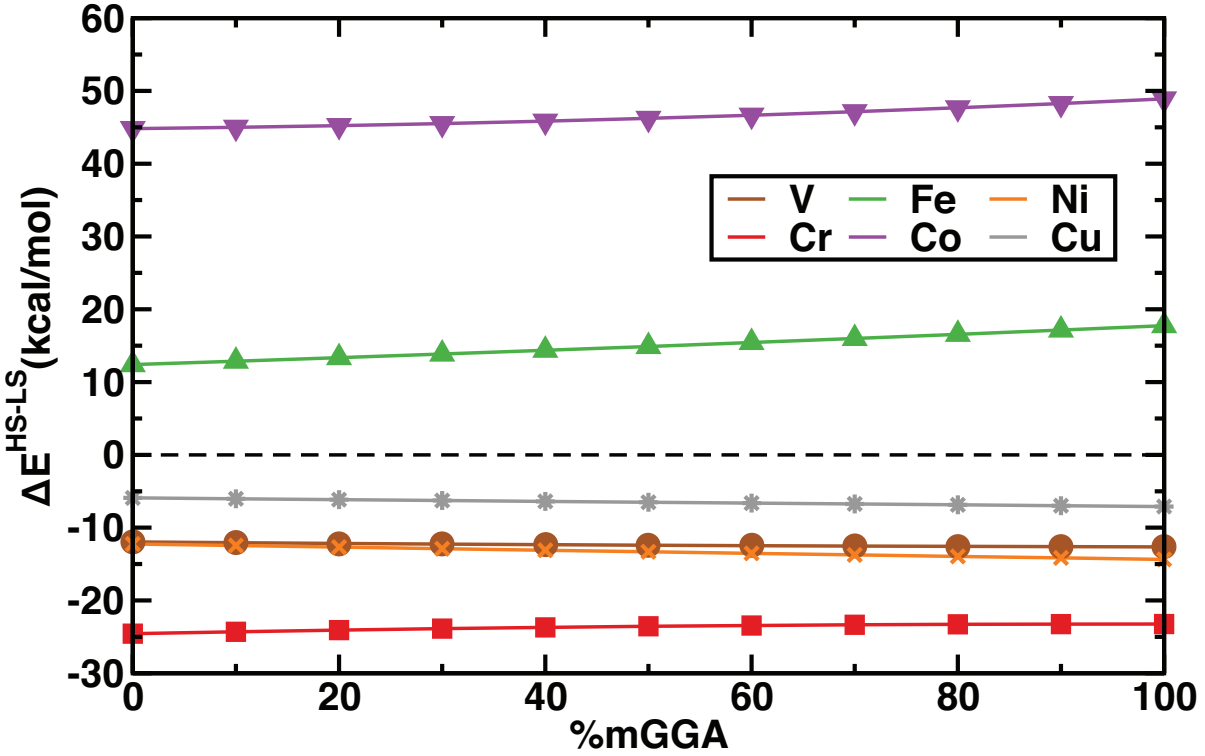

Figure S4. $[M(NH_3)_6]^{3+}$ splittings with percentage of meta-GGA exchange.

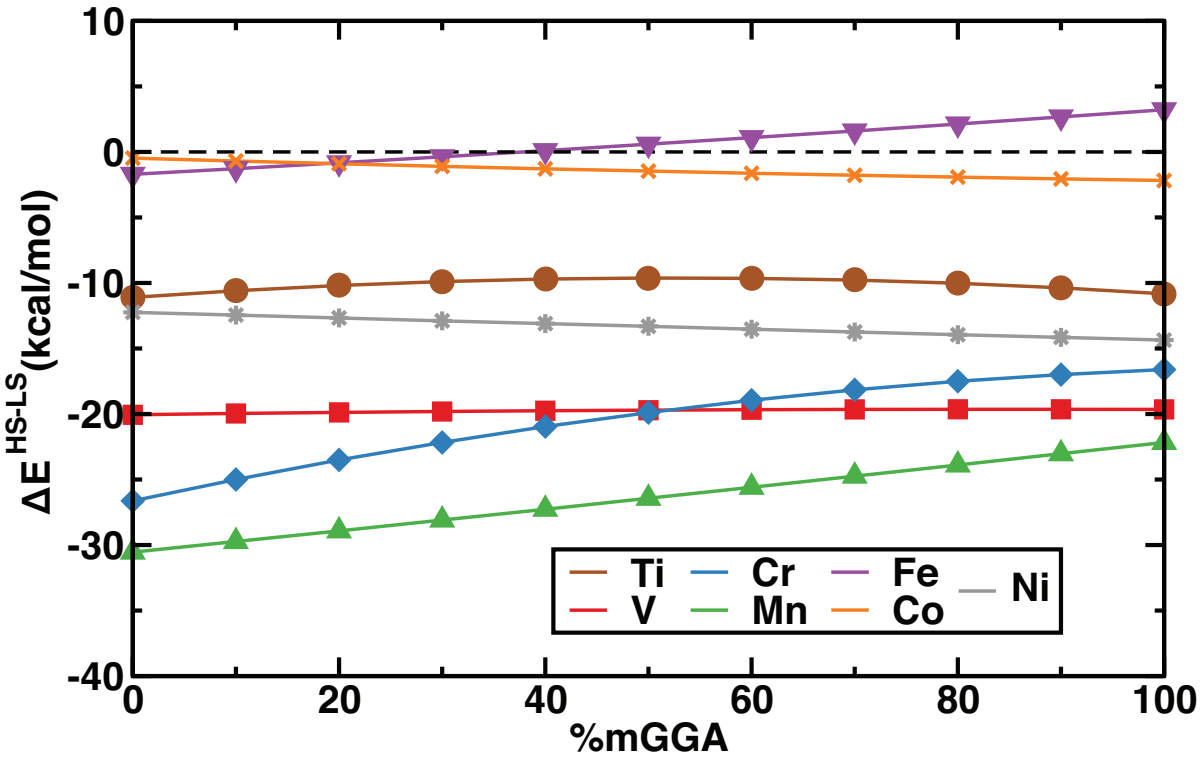

Figure S5. $[M(NH_3)_6]^{2+}$ splittings with percentage of meta-GGA exchange.

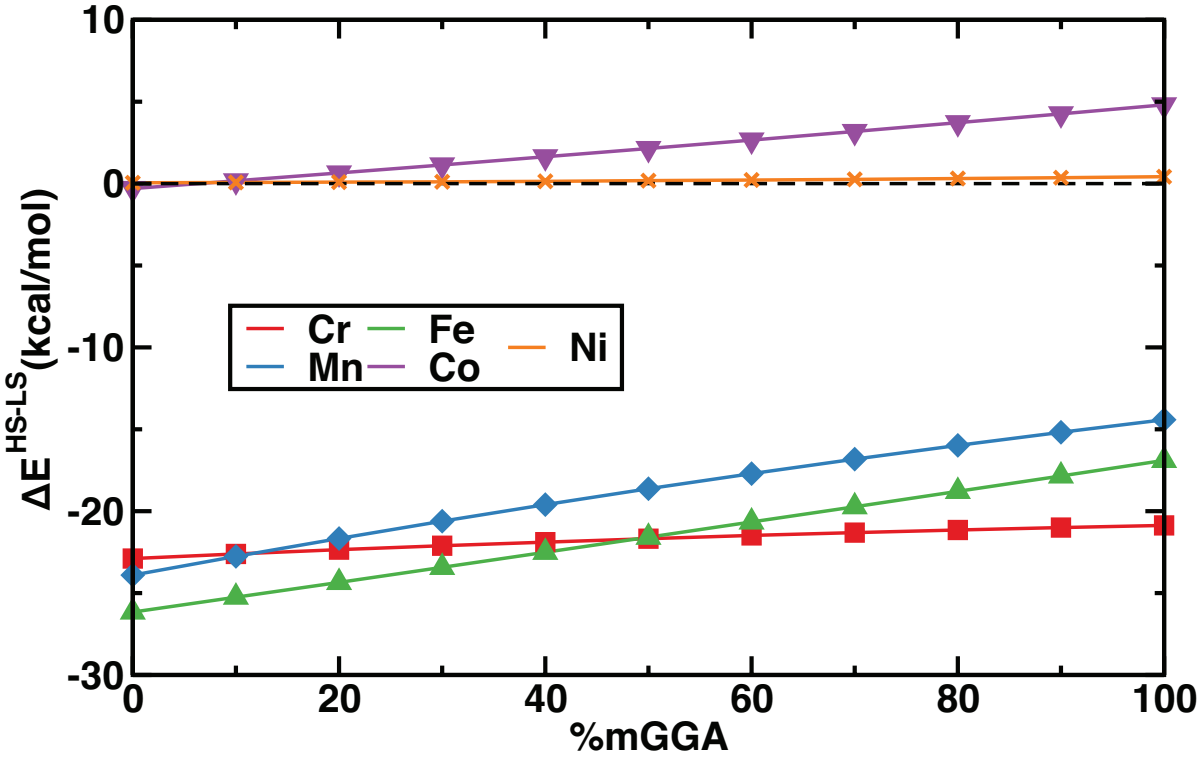

Figure S6. $[M(H_2O)_6]^{3+}$ splittings with percentage of meta-GGA exchange.

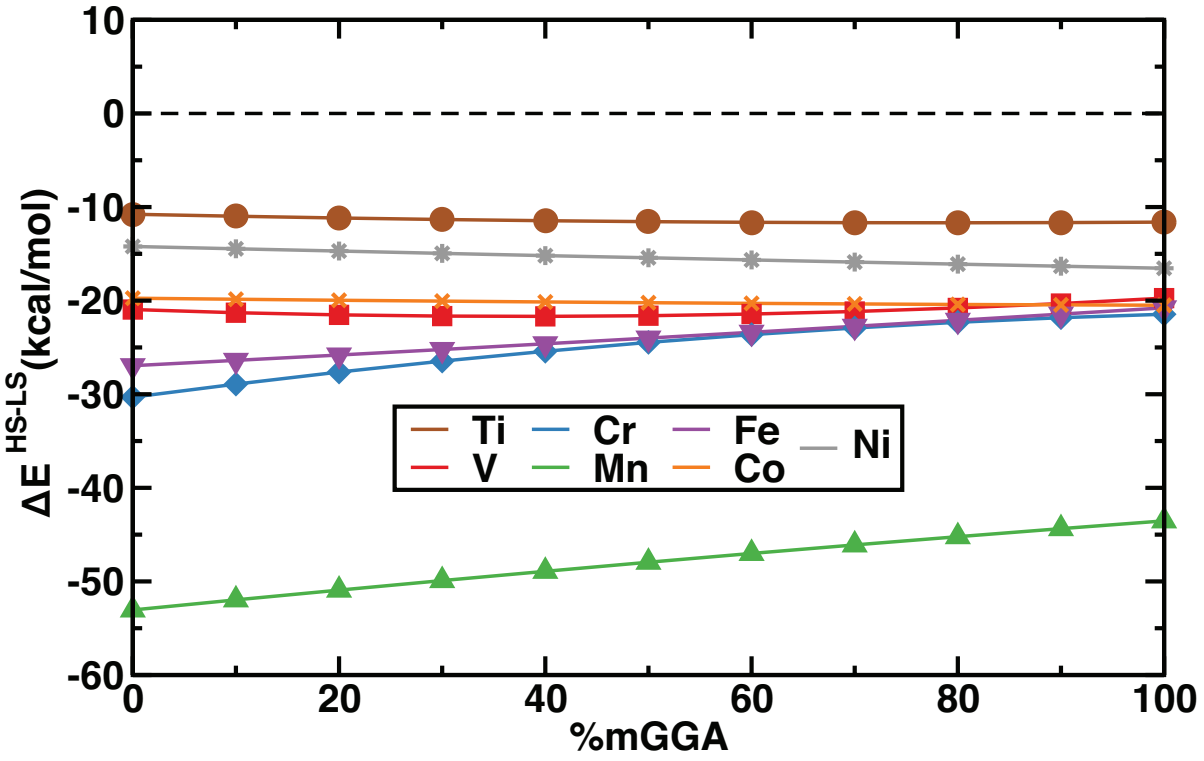

Figure S7. $[M(H_2O)_6]^{2+}$ splittings with percentage of meta-GGA exchange.

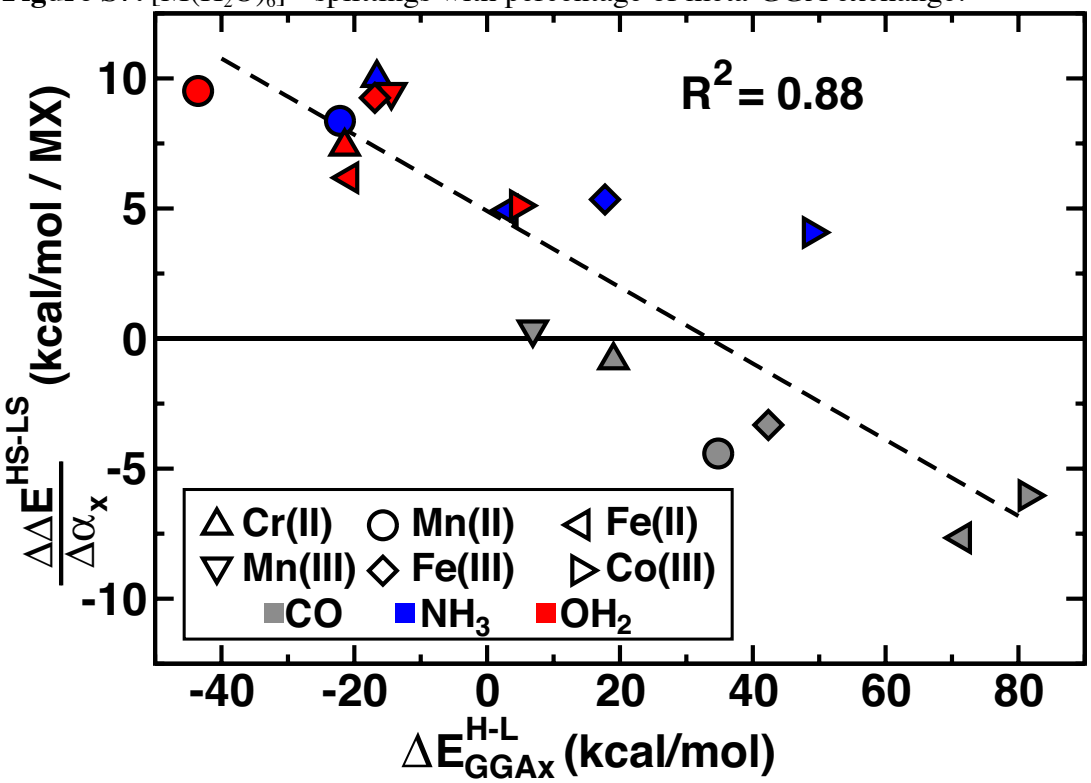

Figure S8. Correlation of mid-row transition metal complex meta-GGA exchange dependence with spin state splittings from GGA.

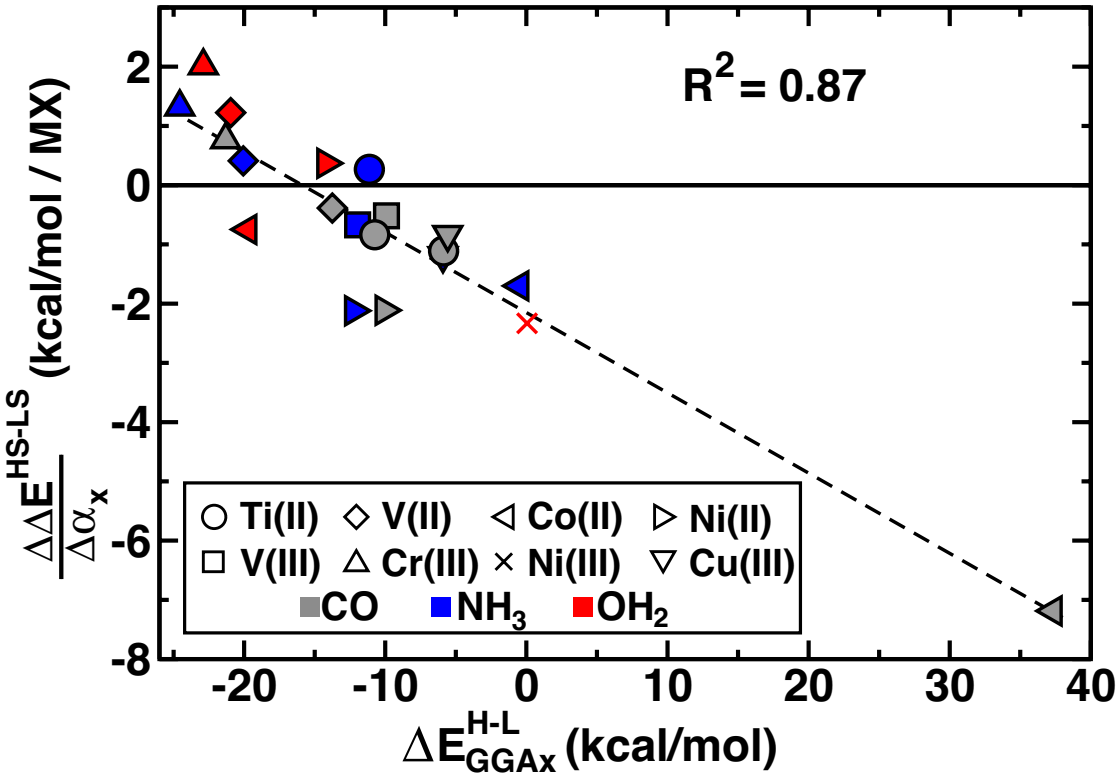

Figure S9. Correlation of early- and late- transition metal complex meta-GGA exchange dependence with spin state splittings from GGA.

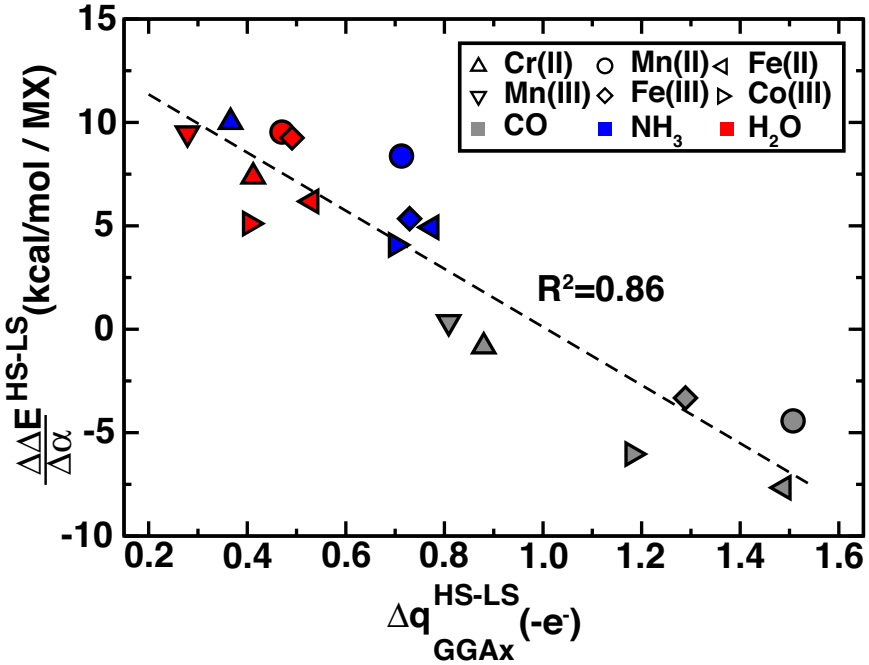

Figure S10. Correlation of midrow transition metal complex meta-GGA exchange dependence with difference in metal partial charge between high-spin and low-spin state at 0% meta-GGA exchange.

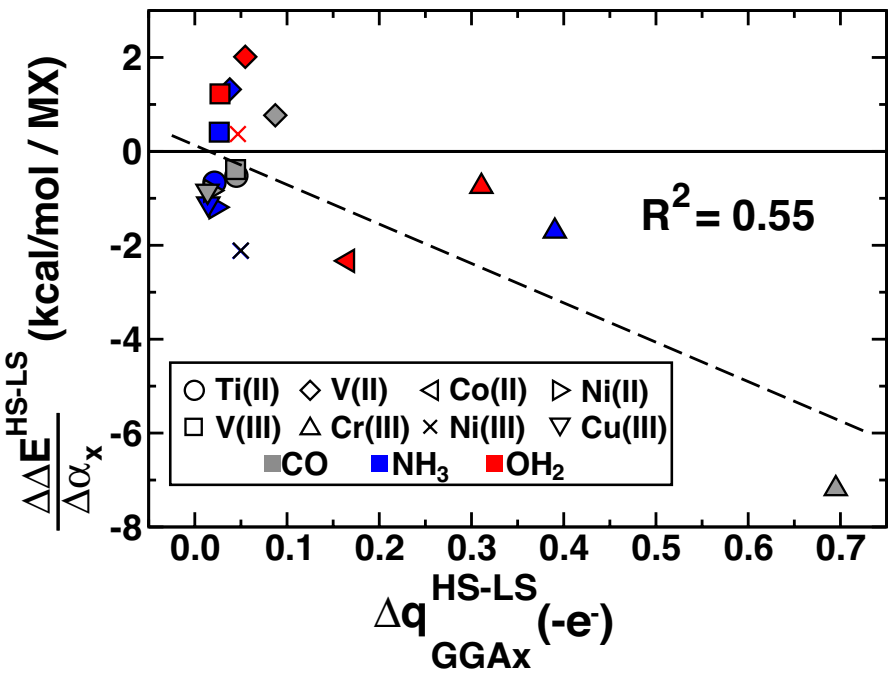

Figure S11. Correlation of early- and late- transition metal complex meta-GGA exchange dependence with difference in metal partial charge between high-spin and low-spin state at 0% meta-GGA exchange.

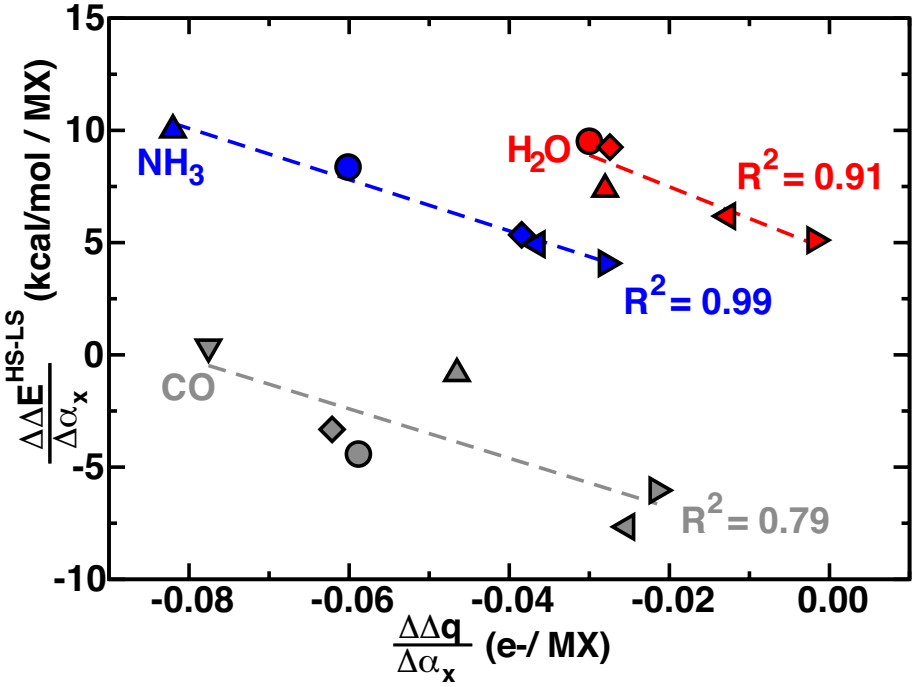

Figure S12. Correlation of mid-row transition metal complex meta-GGA exchange dependence with partial charge difference exchange dependence. The symbols are the same as those indicated in the legend of Figure S9.

Table S58. Slopes, intercepts and R^2 values of the linear regression approximation for the partial derivative of spin-state splitting with meta-GGA exchange (a_x) against the linear regression approximation for the derivative of the difference in the NBO charges between high-spin and low-spin states with a_x. Results are grouped by ligand and correspond to mid-row transition metal complexes.

Ligand	Slope (kcal/mol/MX)	Intercept (e^-/MX)	R^2
CO	-109.9	-9.0	0.79
NH_3	-114.1	0.9	0.99
OH_2	-141.3	4.6	0.91

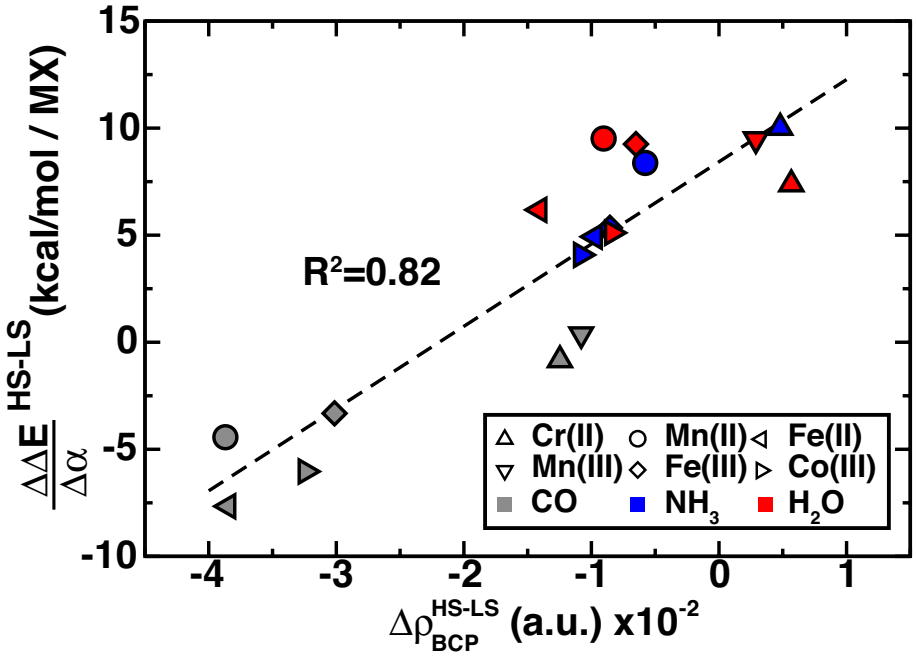

Figure S13. Correlation of mid-row transition metal complex meta-GGA exchange dependence with difference in density at the bond-critical point between high-spin and low-spin states.

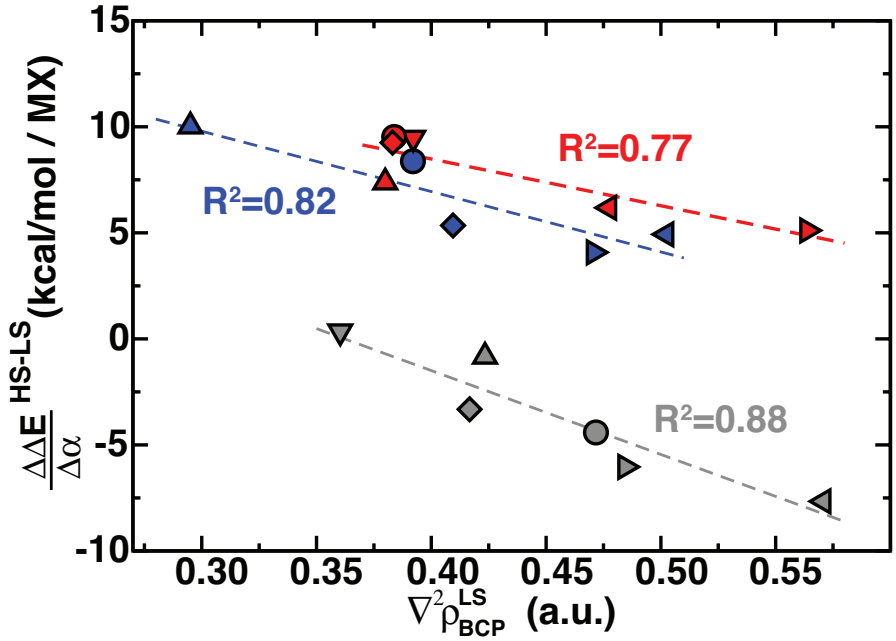

Figure S14. Correlation of mid-row transition metal complex meta-GGA exchange dependence with difference in density at the bond-critical point between high-spin and low-spin states.

Text S1. Trends in charge localization measures

In order to quantify the extent of charge localization on the transition metal center, we compute metal partial charges with NBO natural population analysis. The difference in the calculated charge between the HS and the LS state represents the relative charge-localization between the states,

$$\Delta q^{\text{HS-LS}} = q_{\text{M}}^{\text{HS}} - q_{\text{M}}^{\text{LS}} \ . \tag{1}$$

A positive $\Delta q^{\text{HS-LS}}$, which we will refer to as the charge shift, corresponds to a net loss of electrons (an increase in positive partial charge) on the metal center from the LS to the HS state. For all complexes considered, increasing a_x increases the magnitude of an already positive metal

partial charge for both HS and LS states with an effective delocalization of electron density from the metal to the neighboring ligands. Alternatively, this effect may be viewed as electron localization but onto the ligand, not onto the metal. Despite differences between HF exchange and meta-GGA exchange tuning behavior on energetics, the ligand-centered electron localization observed here is consistent with our previous HF exchange tuning study[6].

The spin-state energetics dependence on meta-GGA exchange and charge shift from LS to HS state at 0% meta-GGA exchange ($\Delta q_{@0\%}^{\text{HS-LS}}$) are well correlated ($R^2$=0.86) for the mid-row (Cr(II)-Co(III)) octahedral complexes and the larger complexes (Figure S9). Weaker correlations are observed for early- and late-row complexes due to the diminished effect of mGGA exchange in these cases (Figure S10). The increase in positive partial charge from LS to HS is greater for the carbonyl complexes (ca. 0.8-1.6 e^- loss), followed by the ammonia (ca. 0.35-0.75 e^- loss) and water complexes (ca. 0.25-0.5 e^- loss). The spin-state splitting sensitivity, $\frac{\Delta\Delta E^{\text{HS-LS}}}{\Delta a_x}$, becomes more negative as the charge shift, $\Delta q_{@0\%}^{\text{HS-LS}}$, increases. The resulting linear-scaling relation from the least squares fit is

$$\frac{\Delta\Delta E^{\text{HS-LS}}}{\Delta a_x} = -14.1\Delta q_{@0\%}^{\text{HS-LS}} + 14.2\,, \tag{2}$$

where the units of this expression are kcal/mol/HFX. The stationary point (i.e. $\frac{\Delta\Delta E^{\text{HS-LS}}}{\Delta a_x} = 0$) of this relationship may be interpolated to occur at a $\Delta q_{@0\%}^{\text{HS-LS}}$ of ~1 e^-, indicating that if the HS state has one less electron localized on the metal with respect to the LS state, then the HS-LS energy splitting will be invariant to meta-GGA exchange. Carbonyl complexes of Cr(II) or Mn(III) reside the closest to that stationary point with a $\Delta q_{@0\%}^{\text{HS-LS}}$ of 0.85-0.9 e^- and negligible spin-state

splitting sensitivity to a_x. In the weak-field ligand complexes studied here (e.g. NH_3, OH_2), $\Delta q_{@0\%}^{\text{HS-LS}}$ is always less than 0.7 e^- with smaller values corresponding to increasing $\frac{\Delta\Delta E^{\text{HS-LS}}}{\Delta a_x}$ and stabilization of LS states.

In addition to a metal-centered view, we may interpret differences in meta-GGA sensitivity through bond-centered metrics. We compared the average electron density difference between HS and LS state at the metal-ligand BCPs for 0% meta-GGA exchange:

$$\Delta\rho_{\text{BCP}}^{\text{HS-LS}} = \rho_{\text{BCP}}^{\text{HS}} - \rho_{\text{BCP}}^{\text{LS}} \quad , \tag{3}$$

where $\rho_{\text{BCP}}^{\text{HS}}$ is the electron density at the metal-ligand BCPs averaged over all metal-ligand bonds for the HS state calculated at 0% meta-GGA exchange and $\rho_{\text{BCP}}^{\text{LS}}$ the corresponding quantity for the LS state. Electron density decrease on the metal ligand bond from LS to HS is greatest for strong-field ligand CO cases (ca. 0.01-0.04 a.u. loss, (Figure S12). In contrast to CO, complexes with weak-field ligands (NH_3, OH_2) show smaller and more varied $\Delta\rho_{\text{BCP}}^{\text{HS-LS}}$ from -0.01 to 0.01 a.u.. The only complexes that have an increase in bonding density in the HS state over the LS state are $Cr(II)(OH_2)_6$, $Cr(II)(NH_3)_6$, and $Mn(III)(OH_2)_6$ where the metal–ligand bond length increases from LS to HS complexes only by 0.08 Å, 0.14 Å, and 0.07 Å, respectively, compared to a larger increase (> 0.10 Å for OH_2 and > 0.20 Å for NH_3) for the corresponding complexes of the other metals. The small number of unpaired electrons in these complexes (d^4 electron configuration) results in empty anti-bonding orbitals for both HS and LS states that correspond to small elongation of the M-L bond length. The good correlation (R^2=0.82) of $\Delta\rho_{\text{BCP}}^{\text{HS-LS}}$ with $\frac{\Delta\Delta E^{\text{HS-LS}}}{\Delta a_x}$ suggests that a large relative density accumulation at the BCPs for LS

states results in stabilization of HS states with increasing a_x, whereas smaller $\Delta\rho_{\mathrm{BCP}}^{\mathrm{HS\text{-}LS}}$ values correspond to stabilization of LS states as meta-GGA exchange is increased. Using a linear best fit:

$$\frac{\Delta\Delta\mathrm{E}^{\mathrm{HS\text{-}LS}}}{\Delta a_x} = 384.1\Delta\rho_{\mathrm{BCP}}^{\mathrm{HS\text{-}LS}} + 8.4 \tag{4}$$

we may predict a $\Delta\rho_{\mathrm{BCP}}^{\mathrm{HS\text{-}LS}}$ that corresponds to meta-GGA exchange invariant structures to be -0.02 a.u.. Increased electron density at the BCP indicates stronger bonding and thus the negative $\Delta\rho_{\mathrm{BCP}}^{\mathrm{HS\text{-}LS}}$ values calculated for most complexes indicate that bonding is consistently weaker in HS than LS complexes, consistent with elongated HS bonds. However, extrapolation of these correlations beyond the surveyed compounds was not possible with the calculated $\Delta\rho_{\mathrm{BCP}}^{\mathrm{HS\text{-}LS}}$ values in the range of -0.04 to -0.02 a.u. for the larger complexes and no strong correlation with their corresponding $\frac{\Delta\Delta\mathrm{E}^{\mathrm{HS\text{-}LS}}}{\Delta a_x}$.

We also examine the sensitivity of the charge shift, $\Delta q^{\mathrm{HS\text{-}LS}}$, to meta-GGA exchange($a_x$) as an indication of how meta-GGA exchange alters the relative HS-LS electronic properties:

$$\frac{\Delta q^{\mathrm{HS\text{-}LS}}}{\Delta a_x} \approx \frac{\partial \Delta q^{\mathrm{HS\text{-}LS}}}{\partial a_x} \quad , \tag{5}$$

where this approximation is again obtained from the slope of a linear regression fit of the charge shift with a_x. Negative (positive) values for the charge difference derivative approximation, $\frac{\Delta q^{\mathrm{HS\text{-}LS}}}{\Delta a_x}$, indicate that the charge difference between HS and LS states decreases (increases) with

increasing a_x. Negative $\frac{\Delta q^{\text{HS-LS}}}{\Delta a_x}$ values are observed in all cases (Figure S11) ranging from -0.08 to -0.01 $\frac{-\text{e}^-}{\text{MX}}$, which corresponds to LS states having stronger charge shift sensitivity to meta-GGA exchange. Therefore, we may determine whether this effect is additive with a frozen-density effect of meta-GGA exchange on spin-state splittings. Starting from $\frac{\Delta q^{\text{HS-LS}}}{\Delta a_x} \approx 0$ and moving toward decreasing $\frac{\Delta q^{\text{HS-LS}}}{\Delta a_x}$, the density difference is additive to the effect of meta-GGA exchange for CO complexes with $\frac{\Delta\Delta\text{E}^{\text{HS-LS}}}{\Delta a_x} < 0$ in all cases, whereas the two effects are opposing for weak-field ligands (NH_3, OH_2) with $\frac{\Delta\Delta\text{E}^{\text{HS-LS}}}{\Delta a_x} > 0$ for all $\frac{\Delta q^{\text{HS-LS}}}{\Delta a_x} < 0$. These two opposing effects serve to further stabilize the LS state in weak-field octahedral complexes.

References

1. Sun, J.; Ruzsinszky, A.; Perdew, J. P., Strongly Constrained and Appropriately Normed Semilocal Density Functional. *Phys. Rev. Lett.* **2015,** *115*, 036402.

2. Shao, Y.; Gan, Z.; Epifanovsky, E.; Gilbert, A. T. B.; Wormit, M.; Kussmann, J.; Lange, A. W.; Behn, A.; Deng, J.; Feng, X.; Ghosh, D.; Goldey, M.; Horn, P. R.; Jacobson, L. D.; Kaliman, I.; Khaliullin, R. Z.; Kuś, T.; Landau, A.; Liu, J.; Proynov, E. I.; Rhee, Y. M.; Richard, R. M.; Rohrdanz, M. A.; Steele, R. P.; Sundstrom, E. J.; Woodcock, H. L.; Zimmerman, P. M.; Zuev, D.; Albrecht, B.; Alguire, E.; Austin, B.; Beran, G. J. O.; Bernard, Y. A.; Berquist, E.; Brandhorst, K.; Bravaya, K. B.; Brown, S. T.; Casanova, D.; Chang, C.-M.; Chen, Y.; Chien, S. H.; Closser, K. D.; Crittenden, D. L.; Diedenhofen, M.; DiStasio, R. A.; Do, H.; Dutoi, A. D.; Edgar, R. G.; Fatehi, S.; Fusti-Molnar, L.; Ghysels, A.; Golubeva-Zadorozhnaya, A.; Gomes, J.; Hanson-Heine, M. W. D.; Harbach, P. H. P.; Hauser, A. W.; Hohenstein, E. G.; Holden, Z. C.; Jagau, T.-C.; Ji, H.; Kaduk, B.; Khistyaev, K.; Kim, J.; Kim, J.; King, R. A.; Klunzinger, P.; Kosenkov, D.; Kowalczyk, T.; Krauter, C. M.; Lao, K. U.; Laurent, A. D.; Lawler, K. V.; Levchenko, S. V.; Lin, C. Y.; Liu, F.; Livshits, E.; Lochan, R. C.; Luenser, A.; Manohar, P.; Manzer, S. F.; Mao, S.-P.; Mardirossian, N.; Marenich, A. V.; Maurer, S. A.; Mayhall, N. J.;

Neuscamman, E.; Oana, C. M.; Olivares-Amaya, R.; O'Neill, D. P.; Parkhill, J. A.; Perrine, T. M.; Peverati, R.; Prociuk, A.; Rehn, D. R.; Rosta, E.; Russ, N. J.; Sharada, S. M.; Sharma, S.; Small, D. W.; Sodt, A.; Stein, T.; Stück, D.; Su, Y.-C.; Thom, A. J. W.; Tsuchimochi, T.; Vanovschi, V.; Vogt, L.; Vydrov, O.; Wang, T.; Watson, M. A.; Wenzel, J.; White, A.; Williams, C. F.; Yang, J.; Yeganeh, S.; Yost, S. R.; You, Z.-Q.; Zhang, I. Y.; Zhang, X.; Zhao, Y.; Brooks, B. R.; Chan, G. K. L.; Chipman, D. M.; Cramer, C. J.; Goddard, W. A.; Gordon, M. S.; Hehre, W. J.; Klamt, A.; Schaefer, H. F.; Schmidt, M. W.; Sherrill, C. D.; Truhlar, D. G.; Warshel, A.; Xu, X.; Aspuru-Guzik, A.; Baer, R.; Bell, A. T.; Besley, N. A.; Chai, J.-D.; Dreuw, A.; Dunietz, B. D.; Furlani, T. R.; Gwaltney, S. R.; Hsu, C.-P.; Jung, Y.; Kong, J.; Lambrecht, D. S.; Liang, W.; Ochsenfeld, C.; Rassolov, V. A.; Slipchenko, L. V.; Subotnik, J. E.; Van Voorhis, T.; Herbert, J. M.; Krylov, A. I.; Gill, P. M. W.; Head-Gordon, M., Advances in Molecular Quantum Chemistry Contained in the Q-Chem 4 Program Package. *Mol. Phys.* **2015,** *113*, 184-215.

3. Domingo, A.; Àngels Carvajal, M.; de Graaf, C., Spin Crossover in Fe(II) Complexes: An Ab Initio Study of Ligand Σ-Donation. *Int. J. Quantum Chem.* **2010,** *110*, 331-337.

4. Bolvin, H., D→ D Spectrum and High-Spin/Low-Spin Competition in D6 Octahedral Coordination Compounds: Ab Initio Study of Potential Energy Curves. *J. Phys. Chem. A* **1998,** *102*, 7525-7534.

5. Pierloot, K.; Vancoillie, S., Relative Energy of the High-(T2g5) and Low-(A1g1) Spin States of [Fe(H2O)6]2+, [Fe(NH3)6]2+, and [Fe(Bpy)3]2+: CASPT2 Versus Density Functional Theory. *J. Chem. Phys.* **2006,** *125*, 124303.

6. Ioannidis, E. I.; Kulik, H. J., Towards Quantifying the Role of Exact Exchange in Predictions of Transition Metal Complex Properties. *J. Chem. Phys.* **2015,** *143*, 034104.